



The Magnetospheric Multiscale Mission...

# Resolving Fundamental Processes in Space Plasmas



Report of the NASA Science and Technology  
Definition Team for the Magnetospheric Multiscale  
(MMS) Mission

National Aeronautics and  
Space Administration

**Goddard Space Flight Center**  
Greenbelt, Maryland 20771

## The NASA STI Program Office ... in Profile

Since its founding, NASA has been dedicated to the advancement of aeronautics and space science. The NASA Scientific and Technical Information (STI) Program Office plays a key part in helping NASA maintain this important role.

The NASA STI Program Office is operated by Langley Research Center, the lead center for NASA's scientific and technical information. The NASA STI Program Office provides access to the NASA STI Database, the largest collection of aeronautical and space science STI in the world. The Program Office is also NASA's institutional mechanism for disseminating the results of its research and development activities. These results are published by NASA in the NASA STI Report Series, which includes the following report types:

- **TECHNICAL PUBLICATION.** Reports of completed research or a major significant phase of research that present the results of NASA programs and include extensive data or theoretical analysis. Includes compilations of significant scientific and technical data and information deemed to be of continuing reference value. NASA's counterpart of peer-reviewed formal professional papers but has less stringent limitations on manuscript length and extent of graphic presentations.
- **TECHNICAL MEMORANDUM.** Scientific and technical findings that are preliminary or of specialized interest, e.g., quick release reports, working papers, and bibliographies that contain minimal annotation. Does not contain extensive analysis.
- **CONTRACTOR REPORT.** Scientific and technical findings by NASA-sponsored contractors and grantees.
- **CONFERENCE PUBLICATION.** Collected papers from scientific and technical conferences, symposia, seminars, or other meetings sponsored or cosponsored by NASA.
- **SPECIAL PUBLICATION.** Scientific, technical, or historical information from NASA programs, projects, and mission, often concerned with subjects having substantial public interest.
- **TECHNICAL TRANSLATION.** English-language translations of foreign scientific and technical material pertinent to NASA's mission.

Specialized services that complement the STI Program Office's diverse offerings include creating custom thesauri, building customized databases, organizing and publishing research results . . . even providing videos.

For more information about the NASA STI Program Office, see the following:

- Access the NASA STI Program Home Page at <http://www.sti.nasa.gov/STI-homepage.html>
- E-mail your question via the Internet to [help@sti.nasa.gov](mailto:help@sti.nasa.gov)
- Fax your question to the NASA Access Help Desk at (301) 621-0134
- Telephone the NASA Access Help Desk at (301) 621-0390
- Write to:  
NASA Access Help Desk  
NASA Center for AeroSpace Information  
7121 Standard Drive  
Hanover, MD 21076-1320

NASA/TM—2000—209883



The Magnetospheric Multiscale Mission...  
Resolving Fundamental Processes in Space Plasmas

*Report of the NASA Science and Technology Definition Team for the  
Magnetospheric Multiscale (MMS) Mission*

*S. Curtis, Goddard Space Flight Center, Greenbelt, Maryland*

National Aeronautics and  
Space Administration

**Goddard Space Flight Center**  
Greenbelt, Maryland 20771

---

December 1999

For more information on the Magnetospheric Multiscale Mission contact:  
Steve Curtis, Code 695, NASA Goddard Space Flight Center, Greenbelt, MD 20771  
Steve.A.Curtis@gsfc.nasa.gov (301) 286-9188

Available from:

NASA Center for AeroSpace Information  
7121 Standard Drive  
Hanover, MD 21076-1320  
Price Code: A17

National Technical Information Service  
5285 Port Royal Road  
Springfield, VA 22161  
Price Code: A10

# Table of Contents

Executive Summary

MMS Science and Technology Definition Team Members

1.0 Introduction	1
1.1 <i>Fundamental Plasma Processes: Reconnection, Particle Acceleration, Turbulence</i>	
1.2 <i>MMS: Key Science Questions</i>	
1.3 <i>Mission Concept and Strategy</i>	
2.0 MMS Science Objectives and Measurement Requirements	7
2.1 <i>Reconnection</i>	
2.2 <i>Particle Acceleration</i>	
2.3 <i>Turbulence</i>	
3.0 The MMS Five-Spacecraft Cluster: the Need for Multipoint Measurements	24
3.1 <i>Separating Temporal and Spatial Effects Using MMS</i>	
3.2 <i>Why a Five-Spacecraft Cluster?</i>	
4.0 Instrumentation	25
4.1 <i>Plasma Instrumentation</i>	
4.2 <i>Energetic Particle Detector</i>	
4.3 <i>Electric Field Instrument</i>	
4.4 <i>Magnetometer</i>	
5.0 Phases of the MMS Mission	27
5.1 <i>Phase 1: Dayside Magnetopause/Near-Earth Magnetotail Investigation</i>	
5.2 <i>Phase 2: Near-Earth Neutral Line/Magnetopause Flanks Investigation</i>	
5.3 <i>Phase 3: Distant Magnetotail Studies</i>	
5.4 <i>Phase 4: Magnetopause Skimming/Mid-Tail Investigation Phase</i>	
6.0 MMS Spacecraft Separation Strategies	28
7.0 Orbit Insertion and Formation Flying	28
8.0 The MMS Spacecraft	29
8.1 <i>Spacecraft Configuration</i>	
8.2 <i>Attitude Control System (ACS)</i>	
8.3 <i>Data and Communication System</i>	
8.4 <i>Power System</i>	
8.5 <i>Interspacecraft Ranging and Alarm System (IRAS)</i>	
9.0 Mission Lifetime and Reliability	34
10.0 Mission Schedule	34
Appendix: Selected References	



## Executive Summary

The Magnetospheric Multiscale (MMS) mission is a multiple-spacecraft Solar-Terrestrial Probe designed to study **magnetic reconnection, charged particle acceleration, and turbulence** in key boundary regions of the Earth's magnetosphere. These three processes—which control the flow of energy, mass, and momentum within and across plasma boundaries—occur throughout the universe and are fundamental to our understanding of astrophysical and solar system plasmas. Only in the Earth's magnetosphere, however, are they readily accessible for sustained study through the in-situ measurement of plasma properties and of the electric and magnetic fields that govern the behavior of the plasmas. But despite four decades of magnetospheric research, much about the operation of these fundamental processes remains unknown or poorly understood. This state of affairs is in large part attributable to the limitations imposed on previous studies by their dependence upon single-spacecraft measurements, which are not adequate to reveal the underlying physics of highly dynamic, highly structured space plasma processes.

To overcome these limitations, MMS will employ five co-orbiting spacecraft, identically instrumented to measure electric and magnetic fields, plasmas, and energetic particles. The initial parameters of the individual spacecraft orbits will be designed so that the spacecraft formation will evolve into a hexahedral configuration near apogee, with three spacecraft defining a plane and the two additional spacecraft located above and below that plane. A possible alternative configuration at apogee would place the fifth spacecraft within a tetrahedron defined by the other four, yielding in effect four smaller tetrahedra inside a larger one. In either configuration, the MMS “cluster” will be able to differentiate between spatial and temporal effects and to determine the three-dimensional geometry of the plasma, field, and current structures under study. Adjustable interspacecraft separations—from 10 kilometers up to a few tens of thousands of kilometers—will allow the cluster to probe the microphysical aspects of reconnection, particle acceleration, and turbulence and to relate the observed microprocesses to larger-scale phenomena.\*

In order to sample all of the magnetospheric boundary regions, MMS will employ a unique four-phase orbital strategy involving carefully sequenced changes in the local time and radial distance of apogee and, in the third phase, a change in the inclination of the orbit from 10° to 90°. In the first two phases, the investigation will focus on the near-Earth tail and the subsolar magnetopause (Phase 1; 12  $R_E$  apogee) and on the low-latitude magnetopause flanks and near-Earth neutral line region (Phase 2; apogee increasing from 12 to 30  $R_E$ ). In Phase 3, MMS will use a lunar gravity assist to achieve a deep-tail orbit with apogee at 120  $R_E$  and to effect the inclination change to 90°. In this phase, MMS will study plasmoid evolution and reconnection at the distant neutral line. In the final, high-inclination

phase, perigee will be increased to 10  $R_E$  and apogee reduced to 40  $R_E$ , on the night side, and the MMS cluster will skim the dayside magnetopause from pole to pole, sampling reconnection sites at both low and high latitudes.

The nominal MMS mission has an operational duration of two years. MMS is currently scheduled for launch in September 2006. While some mission-enhancing technologies such as an interspacecraft ranging and alarm system (IRAS) are desirable, no new mission-enabling technologies are required for the successful accomplishment of the MMS science objectives. The MMS development and launch schedule could therefore be accelerated, with launch occurring as early as December 2004.

With its focus on plasma microprocesses and their coupling to larger-scale phenomena, its ability to resolve spatial and temporal effects, and its unique orbital strategy, MMS will build on the successes of such International Solar-Terrestrial Physics missions as Geotail and Polar to raise to a new level of understanding and insight our knowledge of the physics of the Sun-Earth connection.

### Notable Features of the MMS Mission

- MMS will yield fundamental insights into the physics of reconnection, charged particle acceleration, and turbulence—processes of universal importance in cosmic plasmas.
- High temporal and spatial resolution will permit direct observation of microphysical processes, while adjustable interspacecraft distances will allow study of coupling across scales.
- Through high-resolution observations of the physical processes by which energy is transferred from the solar wind to the magnetosphere, MMS will provide detailed insight into the geoeffectiveness of interplanetary disturbances such as coronal mass ejections and co-rotating interaction regions.
- Five spacecraft in a hexahedral configuration for extended periods near apogee will allow spatial and temporal effects to be differentiated and the 3-D geometry and motion of plasma, field, and current structures to be determined.
- Four orbital phases will provide coverage of all key magnetospheric boundary layers and regions, including pole-to-pole skimming of the dayside magnetopause.
- Lunar gravity assists will be used to effect orbit plane change from low to high inclination.
- The initial parameters of the spacecraft orbits will result in formation of the hexahedral configuration at apogee without active maneuvering on the part of the spacecraft.
- The mission can be accomplished with today's technology.

---

\* The focus on plasma microprocesses distinguishes MMS fundamentally from the Cluster II mission, which will study MHD-scale phenomena. In addition, MMS and Cluster II will sample different regions of the magnetosphere.

## MMS Science and Technology Definition Team Members

### *Chair*

J. L. Burch  
Southwest Research Institute  
San Antonio, Texas

D. G. Mitchell  
The Johns Hopkins University  
Applied Physics Laboratory  
Laurel, Maryland

### *MMS Project Scientist*

S. A. Curtis  
NASA Goddard Space Flight Center  
Greenbelt, Maryland

J. M. Quinn  
Space Science Center  
University of New Hampshire  
Durham, New Hampshire

### *MMS Project Formulation Manager*

J. Durning  
NASA Goddard Space Flight Center  
Greenbelt, Maryland

C. T. Russell  
Institute for Geophysics and Planetary Physics  
University of California, Los Angeles  
Los Angeles, California

### *Members*

D. N. Baker  
Laboratory for Atmospheric and Space Physics  
University of Colorado  
Boulder, Colorado

G. L. Siscoe  
Center for Space Physics  
Boston University  
Boston, Massachusetts

R. E. Ergun  
Space Sciences Laboratory  
University of California, Berkeley  
Berkeley, California

B. U. Ö Sonnerup  
Thayer School of Engineering  
Dartmouth College  
Hanover, New Hampshire

S. A. Fuselier  
Lockheed-Martin Advanced Technology Center  
Palo Alto, California

H. E. Spence  
Center for Space Physics  
Boston University  
Boston, Massachusetts

M. Hesse  
NASA Goddard Space Flight Center  
Greenbelt, Maryland

*Solar Terrestrial Probes Program Scientist*  
R. R. Vondrak  
NASA Goddard Space Flight Center  
Greenbelt, Maryland

A. T. Y. Lui  
The Johns Hopkins University  
Applied Physics Laboratory  
Laurel, Maryland

*S-T Probes Geospace Program Scientist*  
J. A. Slavin  
NASA Goddard Space Flight Center  
Greenbelt, Maryland

R. W. McEntire  
The Johns Hopkins University  
Applied Physics Laboratory  
Laurel, Maryland

## 1.0 Introduction

The Magnetospheric Multiscale (MMS) mission will employ five identically instrumented spacecraft, orbiting in hexahedral formation, to conduct definitive investigations of **magnetic reconnection**, **charged particle acceleration**, and **turbulence** in key boundary regions of the Earth's magnetosphere. These three processes—which control the flow of energy, mass, and momentum within and across plasma boundaries—occur throughout the universe and are fundamental to our understanding of astrophysical and solar system plasmas. It is only in the Earth's magnetosphere, however, that they are readily accessible for sustained study through the in-situ measurement of plasma properties and of the electric and magnetic fields that govern the behavior of the plasmas. Through high-resolution measurements by its cluster of spacecraft, whose separations can be varied from 10 km to a few tens of thousands of kilometers, MMS will probe the crucial microscopic physics involved in these fundamental processes, determine the 3-D geometry of the plasma, field, and current structures associated with them, and relate their microscale dimension to phenomena occurring on the mesoscale. By acquiring data simultaneously at multiple points in space, MMS will be able to differentiate between spatial variations and temporal evolution, thus removing the space-time ambiguity that has bedeviled single-spacecraft studies of magnetospheric plasma processes.

MMS is the fourth Solar-Terrestrial Probe, following TIMED, Solar-B, and STEREO and preceding Global Electrodynamics and Constellation, as set forth in the Strategic Plan of NASA's Office of Space Science. This series of missions provides the major strategic thrust of the Sun-Earth Connections program, the goal of which is to understand solar variability and its influence on the Earth and the other planets.

### 1.1 Fundamental Plasma Processes: Reconnection, Particle Acceleration, Turbulence

The great majority of matter in the observable universe exists in a gaseous ionized state known as the **plasma state**. Stars, stellar atmospheres and winds, stellar and extragalactic jets, and the interstellar medium are examples of astrophysical plasmas. In our solar system, the Sun and the solar corona, the interplanetary medium, the magnetospheres and ionospheres of the Earth and

other planets, as well as the ionospheres of comets and certain planetary moons all consist of plasmas.

Plasmas occur over a wide range of densities (from less than 1 particle  $\text{cm}^{-3}$  in the magnetospheric tail lobes to  $>10^{30}$   $\text{cm}^{-3}$  in stellar interiors) and temperatures (from several thousand degrees Kelvin in the Earth's plasmasphere to  $>10^{10}$  K in pulsar magnetospheres). They exist in both collision-dominated and collisionless regimes and may be partially as well as fully ionized. Because they are made up of electrically charged particles, plasmas can carry electric currents and, unlike neutral gases, are strongly influenced by both intrinsic and external electric and magnetic fields. An important feature of the magnetized plasmas in near-Earth space, first pointed out twenty years ago by *Fälthammar et al.* [1978], is their organization into macroscopic regions or "cells" separated by thin boundary layers and characterized by different densities, temperatures, composition, magnetic field topologies, etc. This cellular structure (**Figure 1.1**) is thought to be characteristic of astrophysical plasmas generally.

The boundaries between plasma cells are not impermeable. The three processes that are the focus of the MMS investigation operate at and in these boundary layers, transporting mass, momentum, and energy across them and driving the dynamics of the plasmas within the cells. **Magnetic reconnection** can link the magnetic fields of adjacent cells, allowing the plasmas to flow directly from one cell to another. As in the flow of ordinary gases around obstacles, turbulence is generated at the cellular interfaces and transports momentum rapidly along the thin boundary layers and into the interiors of the cells. Electric fields associated with waves, reconnection, and turbulence are responsible for the **acceleration** of individual plasma ions and electrons within the boundary layers and inside the cells.

As noted above, these three processes—reconnection, particle acceleration, and turbulence—occur universally and are of fundamental importance in astrophysical and solar system plasmas. However, although their fundamental character has long been recognized, much about their operation remains unknown or poorly understood. For each process, the major outstanding problems are outlined in general terms below. In Section 1.2, these problems will be reformulated as specific science questions that MMS will answer.



**Figure 1.1.** These conceptual representations of the heliosphere (the "bubble" formed in the local interstellar medium by the solar wind and the IMF) (left) and the Earth's magnetosphere (right) illustrate the tendency of astrophysical plasmas to organize themselves into large cells, separated by thin boundary layers. Processes occurring in these thin boundaries are responsible for the large-scale dynamics of the system.

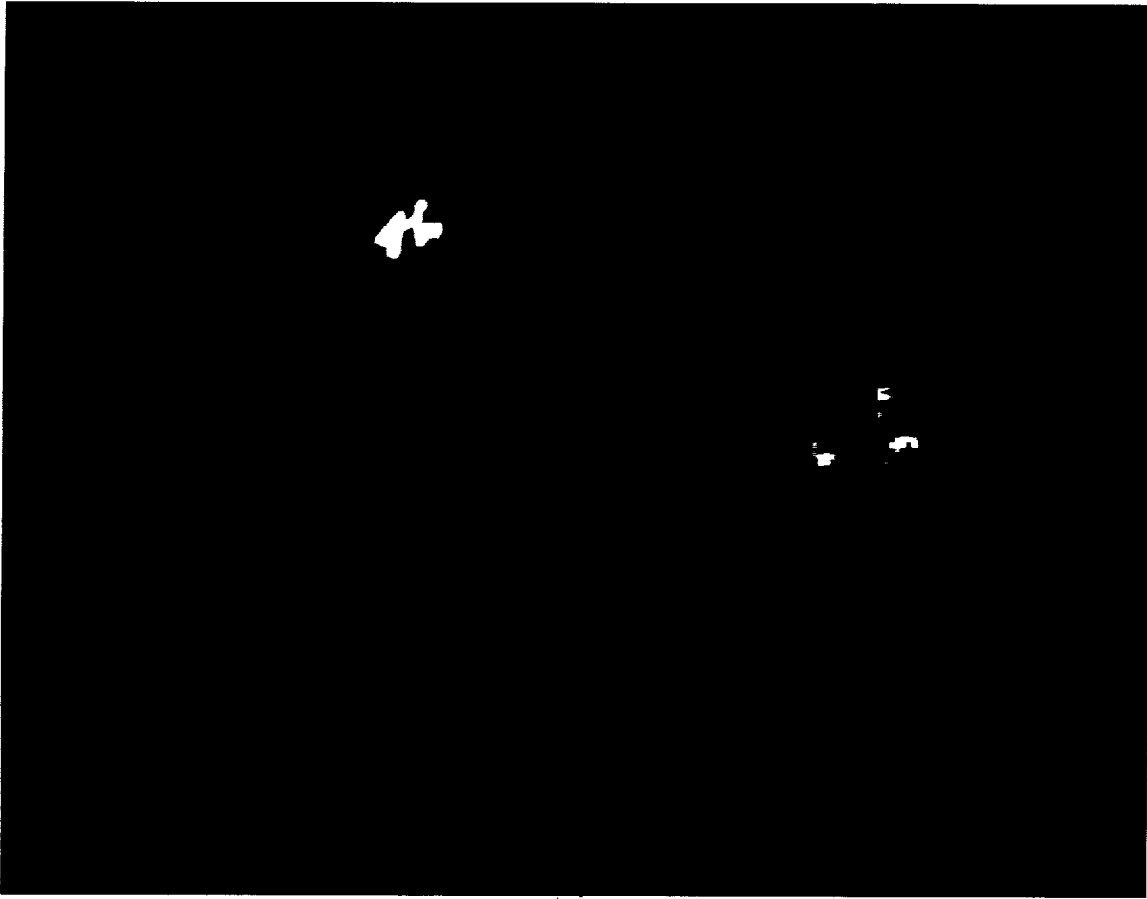


**Figure 1.2.** This TRACE image of EUV emissions from highly ionized iron atoms in the solar corona shows reconnected field lines in a coronal loop. Occurring universally in astrophysical and solar system plasmas, reconnection converts magnetic energy into kinetic particle energy

### 1.1.1 Magnetic Reconnection

In a magnetized plasma, the magnetic field tends to be “frozen” in the plasma by the plasma’s high electrical conductivity, and the plasma and the magnetic flux remain tightly coupled to each other. Abundant evidence exists that this frozen-in condition often breaks down. Magnetic field lines embedded in solar system and astrophysical plasmas then become interconnected, either along their own length or with magnetic fields connected to other bodies. When this interconnection (usually called reconnection or merging) occurs, magnetic field energy is converted to kinetic energy of the plasma ions and electrons, and plasmas can move directly from the environment of one star or planet to another. This process is thought to occur preferentially when the magnetic fields in adjacent plasma domains are oriented opposite—“antiparallel”—to one another.

The reconnection process, whether in collisional plasmas near stellar bodies or in collisionless plasmas within stellar winds and planetary magnetospheres, is thought to be of great importance for energy transfer throughout the universe. For example, recent high-resolution optical images from the TRACE satellite have confirmed that reconnection of magnetic fields in the upper atmosphere of the Sun plays a key role in producing the explosive ejection of solar material outward into the solar system (**Figure 1.2**). Such eruptive events are responsible for great magnetic storms on Earth. Cited as further evidence for the importance of

reconnection is the fact that geomagnetic disturbances occur more frequently and become stronger as the magnetic field in the solar wind becomes more southward and thus more antiparallel to the Earth’s magnetic field. Accelerated plasma flows observed at these times along the boundary of the Earth’s magnetic field and within its extended tail are consistent with the acceleration of charged particles expected to result from magnetic reconnection.

Among the important questions about reconnection that need to be answered are the following:

- Under what conditions can ambient magnetic-field energy be converted to plasma energy by the annihilation of magnetic field through reconnection?
- Does reconnection only occur explosively or can it also be steady?
- What microscale processes are responsible for reconnection?
- How do reconnection processes couple to larger scales?
- What determines the rate of reconnection?
- Why are some magnetic configurations stable and others not?

The regions where reconnection occurs in the Earth’s magnetosphere, mainly the dayside magnetopause and the magnetotail, are easily accessible to Earth-orbiting spacecraft, offering our only



**Figure 1.3.** Two illustrations of particle acceleration in different astrophysical settings. (left) The Crab Nebula—the remnant of a supernova observed in 1054 c.e.—glows from synchrotron radiation emitted by energetic electrons accelerated in the intense magnetic field of the pulsar located at the nebula's center. (right) Energetic electrons accelerated to velocities near the speed of light are also responsible for the synchrotron emission from Jupiter's powerful radiation belts. The false color indicates the intensity of the emission, with red being the most intense. The Crab nebula image is from *Wainscoat and Kormendy* [1997] and is used courtesy of R. J. Wainscoat. The jovian synchrotron figure is from *de Pater et al.* [1997] and is used courtesy of I. de Pater and NRAO/VLA.

opportunity for detailed, close-up observations of this important astrophysical process. Because reconnection is a three-dimensional process involving the rapid inflow and outflow of plasma particles, a cluster of spacecraft with carefully selected separations and instruments will be needed for a definitive experiment.

### 1.1.2 Particle Acceleration

The astrophysical acceleration of charged particles was first recognized in the ground-based measurements of the energy spectra of solar and galactic cosmic rays. Later, radio-wave emissions from relativistic particles and from unstable plasma distributions were found to be the source of astronomical radio emissions, from the Earth's auroral kilometric radiation to those from radio galaxies. Through the interaction of charged particles with the neutral gases surrounding the stars and planets, particle acceleration is responsible for much of the luminosity of gaseous astrophysical bodies and the upper atmospheres of the planets at wavelengths from the ultraviolet to gamma rays (**Figure 1.3**).

Charged particle acceleration can occur directly, for example, by electric fields directed along the magnetic field; stochastically, in association with magnetic clouds, hydromagnetic waves, and shocks; or resonantly, in association with wave-particle interactions. Particle acceleration is linked directly to the other two cornerstone processes. For example, a part of the electric field associated with reconnection is directed along the magnetic field, producing direct particle acceleration. As discussed in the next section, fluid turbulence is associated with stochastic acceleration, while microturbulence is the source of wave-particle interactions, which can produce resonant acceleration.

Important unresolved questions concerning particle acceleration include the following:

- Where and how are charged particles accelerated?
- How is a very small fraction of the ambient charged particles sometimes chosen to receive extremely high energies?
- Is there more than one stage in the acceleration?
- When is an injection process necessary to provide initial acceleration before another process takes over?
- What is the role of time-varying magnetic fields in high-energy particle acceleration?

Experimental capabilities have progressed to the point where direct observations of reconnection electric fields, induced electric fields, plasma waves, and the resulting particle distributions can be used to discriminate among competing theories of particle acceleration. Multipoint measurements with suitable interspacecraft separations are needed to distinguish between temporal and spatial variations of the fields and particles.

### 1.1.3 Turbulence

Astrophysical plasmas fluctuate irregularly in the temporal and spatial domains and hence are turbulent (**Figure 1.4**). Plasma turbulence is typically strong, with the fluctuations of magnetic fields and fluid velocities being comparable to their mean values. Direct observations have shown that astrophysical and geophysical fluids, whether on the surface of the Earth, in planetary atmospheres, or the plasma environments of interplanetary space and the Earth, exhibit power spectra that decrease rapidly toward shorter wavelengths. Remote observations of the interstellar gas and stellar convection zones have revealed strong levels of turbulence with similar spectra.

Fluid turbulence carries momentum and energy that drive plasma motions and, through dissipation, heat the plasma. On smaller



**Figure 1.4.** Turbulent phenomena occur throughout the universe. This computer simulation illustrates the turbulent structure produced by Kelvin-Helmholtz instabilities in an astrophysical jet. (Image courtesy M. L. Norman, National Center for Supercomputing Applications, University of Illinois at Urbana-Champaign)

scales, microturbulence leads to the acceleration and transport of charged particles by interactions with waves in the plasma. These wave-particle interactions can at times be resonant, with the particles absorbing a large fraction of the wave energy, resulting in a transition from weak to strong turbulence. Microturbulence is thought to be driven by kinetic processes associated with magnetic reconnection, shear layers, particle beams, and collisionless shocks. An important aspect of microturbulence is its ability to couple into the larger scale fluid turbulence.

Important unanswered questions about plasma turbulence include the following:

- What is the role of fluid turbulence in transporting mass and momentum across plasma boundary layers?
- What controls the onset of turbulence in thin current sheets?
- What are the sources, propagation, and consequences of mesoscale boundary waves?
- What kinetic processes drive microturbulence?
- How does microturbulence couple into mesoscale disturbances?

The wide range of temporal and spatial scales involved in turbulence requires that multiple spacecraft be used to determine such parameters as growth rates and correlation lengths. Multiple spacecraft are also needed to relate the onset of turbulence in boundary layers to conditions on either side of the boundaries and to trace the propagation and growth of turbulence from the microscale to the mesoscale.

## 1.2 MMS: Key Science Questions

MMS will address a number of unresolved questions relating to each of the three fundamental processes. These questions represent particularizations of the more general plasma-physical questions, applicable to all astrophysical systems, that were set forth in the preceding section. To date, answers to them have remained

elusive, or at best partial, because of the limitations imposed by our dependence on measurements from a single spacecraft at a single point in geospace. Nor, for the most part, will answers be provided by the multipoint data from Cluster II, which will focus on different regions and have larger spacecraft separations appropriate to its main objective of investigating MHD turbulence. (See **Table 1.1** for a comparison of Cluster II and MMS.)

The MMS key science questions are outlined below. These questions, together with the measurements required to answer them, will be discussed in detail in the Section 2.

### 1.2.1 Reconnection

- What are the kinetic processes responsible for collisionless magnetic reconnection, and how is reconnection initiated?
- Where does reconnection occur at the magnetopause and in the magnetotail, and what influences where it occurs?
- How does reconnection vary with time, and what factors influence its temporal behavior?
- How are flux transfer events and plasmoids/magnetotail flux ropes formed, and how do they evolve?

### 1.2.2 Particle Acceleration

- What is the role of inductive electric fields in high-energy particle acceleration?
- What is the cause and structure of plasma injection in the near-Earth tail?
- What are the mechanisms for acceleration of charged particles in plasma boundary layers?

### 1.2.3 Turbulence

- What are the temporal and spatial properties of, and the physical processes responsible for turbulence in the magnetosheath, magnetopause, and plasma sheet?

	Cluster	MMS
Bow shock	X	
Subsolar magnetopause		X
Z-scan of neutral sheet at 20 $R_E$	X	
X-, Y-scan of neutral sheet at 8 to 200 $R_E$		X
Skimming of dayside magnetopause		X
In-out scan of cusp	X	
In-out scan of high-latitude magnetopause	X	
Minimum separation distance	200 km	10 km

**Table 1.1** Comparison of the magnetospheric coverage and spatial resolution achieved with Cluster II and MMS.

- What are the sources, propagation, and consequences of mesoscale boundary waves?
- What is the role of turbulence in plasma entry through the magnetopause?

### 1.3 Mission Concept and Strategy

The boundary regions of the magnetosphere (**Figure 1.5**) comprise a “laboratory” within which MMS will perform definitive experiments on reconnection, particle acceleration, and turbulence as these fundamental plasma processes manifest themselves in the magnetospheric setting. MMS will probe these regions meticulously and systematically with measurements of the key parameters on the necessary spatial and temporal scales and resolutions. Specification of the experimental capabilities of MMS has been guided by results of the latest magnetospheric models and theories of magnetospheric plasma phenomena.

The MMS “laboratory equipment” will consist of five co-orbiting spacecraft identically instrumented to measure electric and magnetic fields, plasmas, and energetic particles. The separation between the spacecraft will be adjustable from 10 km up to a few tens of thousands of kilometers. In order to measure spatial gradients in crucial regions, the individual spacecraft orbits will be trimmed to achieve a hexahedral configuration near apogee, with three of the spacecraft defining a plane and with the two additional spacecraft being located above and below that plane. The apogee configuration can be viewed as two three-sided pyramids joined at their bases with the five spacecraft at the five corners of the structure. Alternatively, the fifth spacecraft could be placed inside a tetrahedron defined by the other four, forming four smaller tetrahedra within a larger one, which would then provide full vector gradients of the derived quantities over a smaller spatial scale. The orbit will be adjustable, allowing the spacecraft “clus-

ter” to sample all of the important boundary layers within the magnetosphere.

The boundary layer sampling requirement leads to another unique aspect of the MMS mission—its four orbital phases. In the first phase, the orbit will be equatorial and highly elliptical, with apogee at 12  $R_E$  on the night side where it will “dwell” in the current disruption region that is responsible for the initiation of magnetospheric substorms. The apogee will precess toward the dayside, reaching the subsolar region where reconnection of the interplanetary and terrestrial magnetic fields occurs. As the apogee precesses back to the night side, its distance will be gradually increased up to 30  $R_E$  at the midnight meridian. In this orbit, MMS will dwell in the substorm reconnection region. Next, MMS will use a lunar gravity assist to achieve a deep tail-orbit with apogee at 120  $R_E$ , where it will investigate the evolution of plasmoids and probe the distant-tail reconnection region. Finally, the orbital inclination will be increased to 90°, and the perigee will be increased to 10  $R_E$  and apogee reduced to 40  $R_E$ , on the night side. This final orbit will skim the dayside magnetopause from pole to pole.

As the MMS spacecraft cluster encounters the various plasma boundary regions, its data acquisition will be guided by plasma models. At the larger scales, MHD models that have been developed and verified as part of the ISTP program will be used to “target” the spacecraft to acquire specific phenomena under the extant conditions. Plasma simulations extending down into the microscale will then be integrated with the spacecraft data in order to validate the models, quantify uncertain parameters, and help identify the “smoking guns,” such as parallel electric fields, electron pressure gradients, and particle acceleration, that will definitively establish what processes control the Earth’s space environment.

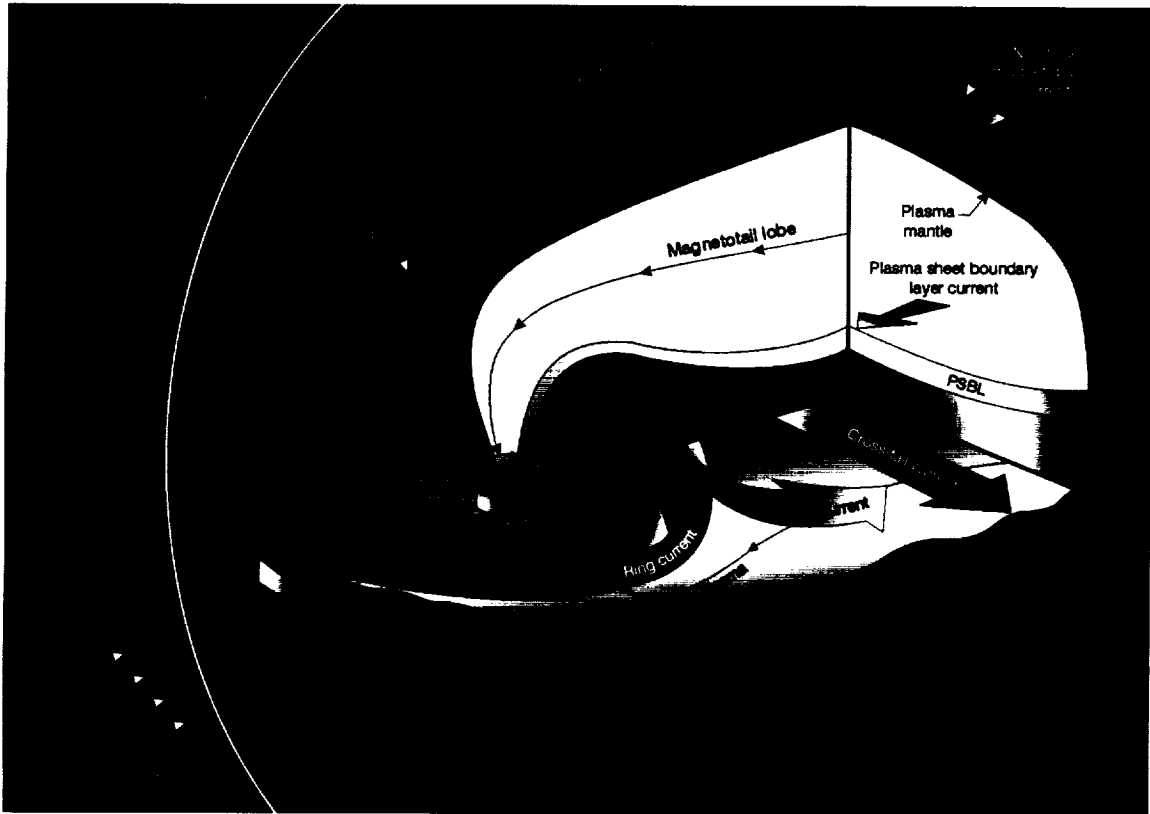


**Figure 1.5.** The Earth's magnetosphere, which has been termed the “fourth geosphere” because it surrounds the lithosphere, hydrosphere, and atmosphere, epitomizes the cellular structure of space plasmas discussed in Section 1.1. It is made up of abundant examples of magnetically organized structures and their boundary layers, which frequently harbor dynamic phenomena (particle acceleration, magnetic merging, explosive energy transformation, turbulent flows, and the spontaneous generation of mesoscale structures). The thin boundary separating the magnetosphere from its surrounding plasma environment, the solar wind, is a distinctive feature called the magnetopause, inside of which is a thicker boundary layer where plasmas from inside and outside are mixed. The magnetosphere itself is a composite of cells, including both permanent structures such as the two tail lobes and the plasma sheet that separates them and transient structures such as plasmoids—disconnected segments of the plasma sheet ejected down the tail during substorms.

## 2.0 MMS Science Objectives and Measurement Requirements

The prime objective of the MMS mission is to explore and understand reconnection, particle acceleration, and turbulence on the micro- and mesoscale in the Earth's magnetosphere. Achievement of this objective will allow the determination of how energy, mass, and momentum are transferred from the solar wind to the magnetosphere. At the same time, it will clarify greatly how these same processes act in other astrophysical contexts. Specific science objectives, defined in terms of the key science questions outlined in the Section 1.2, are discussed below, along with the measurements and orbital strategies that MMS will employ to achieve them.

### 2.1 Reconnection

Substantial evidence, both direct and indirect, exists for the occurrence of reconnection at the magnetopause and in the magnetotail and for the crucial role that it plays in the topology and dynamics of the magnetosphere (**Figure 2.1**). Analytical studies and numerical simulations have contributed important insights into the physics of reconnection. However, many fundamental questions remain to be answered: What processes allow recon-

nection to occur in a collisionless regime? What are the roles of non-MHD processes (such as kinetic Alfvén waves, whistler waves, and electron inertial effects) in reconnection? What is the size and three-dimensional structure of the reconnection diffusion region? At what rate does reconnection occur and over what interval of time? Under what conditions is reconnection quasi-continuous? episodic? What is the spatial distribution and morphology of reconnection sites on the magnetopause and in the tail? What factors control the occurrence, rate, location, and temporal variability of reconnection?

MMS high-resolution plasma and fields data—acquired at multiple points in space, over a range of spatial scales (**Table 2.1**), and at both high and low latitudes—will make it possible to answer such outstanding questions, which address various aspects of the four key reconnection questions listed in Section 1.2.1. The answers that MMS provides will ultimately reveal how the magnetosphere is controlled by the solar wind and will at the same time yield a basic understanding of how and why reconnection proceeds in a collisionless plasma. Particularly exciting is the prospect that, owing to its high spatial resolution (~10 km interspacecraft separation), MMS will be able observe directly the microphysical processes that lead to the breakdown of the frozen-in-flux constraint and allow reconnection to occur.

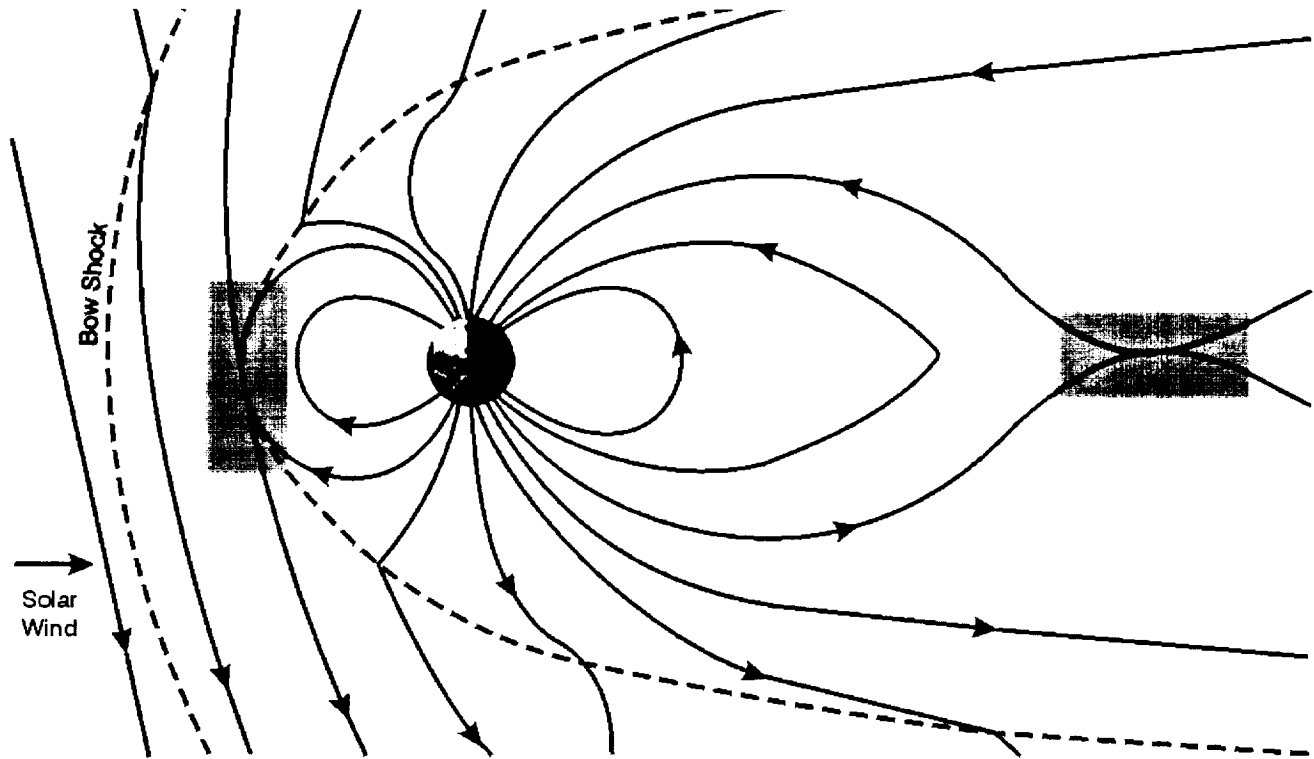


**Figure 2.1.** Southward-oriented interplanetary magnetic field (IMF) lines (blue) merge or reconnect with the Earth's closed field lines (green) at the subsolar point. The merged or "open" flux tubes (red), with one end in the Earth's ionosphere and the other end in the solar wind, are carried downstream by the solar wind flow and eventually reconnect in the distant tail. Merging results from the breaking of the frozen-in-flux condition, which occurs at an X-line in the diffusion or dissipation region (grey boxes). Merging of closed field lines in the near-Earth region of the magnetotail (not shown here) is associated with the substorm expansion phase. Reconnection at the dayside magnetopause is the primary mechanism for the transfer of mass, momentum, and energy from the solar wind to the magnetopause, which occurs most efficiently when the IMF is oriented southward. In the tail, merging plays a role in the dissipation of energy stored in the magnetotail lobes as a result of dayside reconnection. (The drawing is not to scale.)

Scale	<i>Global</i>	<i>Large (MHD)</i>	<i>Intermediate</i>	<i>Electron Pressure Gradient</i>	<i>Electron Inertia</i>
<b>Typical Length</b>	Many Earth radii	Earth radii	Few to one ion inertial length (~few 100 km)	Between ion and electron inertial scales (~10s to 100s km)	Electron inertial length (~10s of km)
<b>Signatures</b>	Polar cap growth, shrinking	Fast flows associated with magnetic field components normal to current sheet	Ion-electron decoupling, faster electron flow (up to multiples of Alfvén speed) than ion flow  Electron flow more localized  Quadrupolar current-aligned magnetic field signature around reconnection site	Nongyrotropic electron pressure anisotropies of a few % of isotropic pressure  Electron current sheet with width less than ion inertial length	Strong electron current fluctuations and very short bursts
<b>Evidence</b>	Data, theory	Data, theory, MHD simulations	Hall MHD, hybrid and fully electromagnetic particle simulations, theory	Modified hybrid and full particle simulations	Modified hybrid and particle simulations, analytical theory

**Table 2.1** Reconnection is a multiscale process. At the largest scales, spacecraft data have confirmed the predictions of magnetohydrodynamic theory. Numerical modeling studies have now begun to focus on the smaller-scale, kinetic regime, and higher-resolution data from multiple locations surrounding the reconnection site are needed to validate the results of these studies.

### 2.1.1 What Are the Kinetic Processes Responsible for Collisionless Magnetic Reconnection? How Is Reconnection Initiated?

Magnetic reconnection relies on the presence of a region in which dissipative electric fields are generated and the frozen-in-flux condition breaks down. This region is known as the “diffusion” or “dissipation” region. It is very localized, lying within the gyroradius of protons in the weak magnetic fields near the magnetopause or near the central current sheet of the geomagnetic tail.

The occurrence of reconnection has been established through the detection of large-scale signatures such as magnetic flux transfer, fast plasma flows, plasma heating, and energetic particle acceleration at the dayside magnetopause and in the tail plasma sheet. With one possible exception, however, the reconnection site itself—the diffusion region—has not been directly observed or, at least, its properties have not been clearly identified in spacecraft data. There are two reasons for this lack of direct observations. First, the localization of the diffusion region and of the processes acting therein requires fast plasma instrumentation, which has not been available until recently. Second, theoretical understanding of the physics of the dissipation region was not sufficiently developed to predict data signatures that would be indicative of an encounter with the diffusion region. Recent theoretical and modeling efforts, however, have made great progress toward describing the inner workings of reconnection in collisionless plasmas and have specified observational signatures diagnostic of the mechanisms responsible for the breaking of the frozen-in-flux condition. Guided by these models and equipped with fast instrumentation, MMS will be able to identify and probe reconnection

sites at the magnetopause and in the tail and will acquire the data needed to validate our theoretical picture of the microprocesses responsible for reconnection.

Our present understanding of magnetic reconnection can be summed up as follows: The diffusion region proper consists of two embedded regions of different physical parameters and sizes (**Figure 2.2**). The larger, called the “Hall zone,” exhibits typical dimensions of a few to about ten ion inertial lengths, which in many cases is roughly equivalent to the ion gyroradius. In typical space plasmas this dimension is a few hundreds of kilometers. Here the larger ion mass generates a region where the ions decouple from the electrons. The resulting currents are consistent with a quadrupolar out-of-plane magnetic field structure roughly aligned with the reconnection line, also called the X-line.

The inner diffusion region is dominated by electron physical processes. These generate the reconnection electric field, which is also aligned with the X-line and hence has a component parallel to the magnetic field, thereby violating the frozen-in-flux constraint. This electric field can be generated by bulk electron acceleration in the direction antiparallel to the main current flow or by nongyrotropic electron pressure anisotropies. The former mechanism appears to dominate in the case of very thin (~electron inertial length) current sheets or in the presence of a guide magnetic field and is likely to occur at the magnetopause. In the case of thick (~ion inertial length) current sheets, it is the nongyrotropic electron pressure tensor that is responsible for the generation of the reconnection electric field. Which mechanism operates may be determined by such external factors as the rate at which the magnetotail current sheet thins.

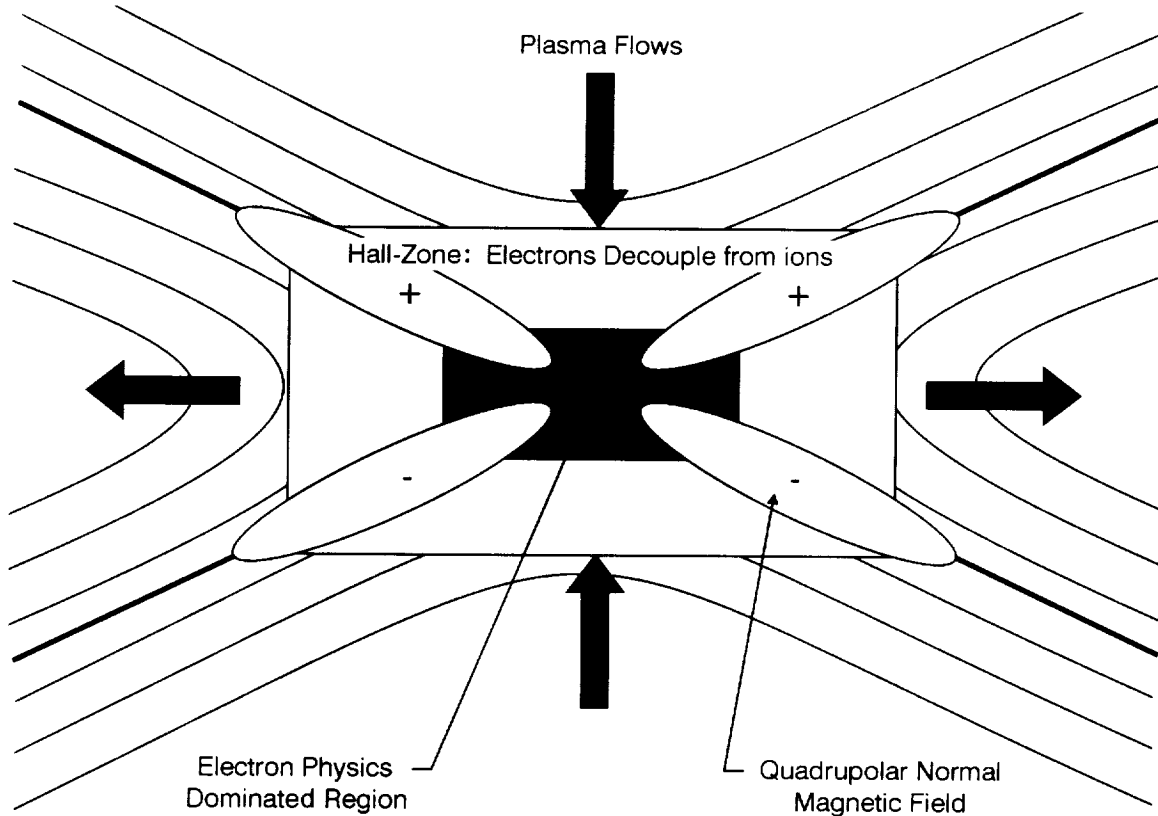


**Figure 2.2.** Reconnection occurs within a spatially limited region known as the dissipation or diffusion region, illustrated schematically here by the large rectangular box. Recent analytical studies suggest that the diffusion region consists of an outer region, where the ions are demagnetized but the electrons remain coupled to the magnetic field, and an inner region near the X point, where the electrons become demagnetized as well, breaking the frozen-in-flux condition and allowing reconnection to proceed. The heavy lines in the drawing represent the “separatrices,” field lines that separate regions of different magnetic topology. Plasma flows into the diffusion region from both sides of the separatrix, carrying with it the frozen-in magnetic flux. As the frozen-in condition is broken and the fields merge, plasmas from the separate domains mix along reconnected field lines and are accelerated away from the diffusion region in the outflow regions. Detection of accelerated flows on the magnetopause and in the tail provides strong evidence for the occurrence of reconnection.

In addition to probing the microscale mechanisms inside the diffusion region that operate once reconnection has begun, MMS will also address outstanding questions about kinetic processes involved in the onset of reconnection. For example, in the case of the magnetotail, observations as well as recent modeling results suggest that the formation of thin strong current sheets and a reduction of the normal magnetic field during the substorm growth phase may be a necessary precondition for the occurrence of reconnection. The reduction in  $B_z$ , which is necessary to maintain the strong current density, results in the electrons becoming “unfrozen” from the magnetic field and thus makes possible the onset of reconnection. The demagnetization of the electrons is a small-scale, kinetic process, involving either direct particle motion or possibly wave-particle interactions, that can be resolved and investigated by the MMS cluster.

Finally, MMS, with its hexahedral formation and adjustable interspacecraft distances, is ideally suited to study the three-dimensional nature of magnetic reconnection, about which little is known. Of particular interest is the influence of modes with wave vectors in the (cross-tail) current direction and of the turbulence associated with these modes on the initiation and evolution of the reconnection process and on its effectiveness on large scales.

## **2.1.2 Where Does Reconnection Occur at the Magnetopause and in the Magnetotail, and What Influences Where It Occurs?**

**2.1.2.1 Magnetopause.** The observational foundation for our picture of reconnection at the magnetopause consists largely of a limited number of discrete in-situ observations at low and middle latitudes and in the cusp. These data indicate that reconnection occurs at low latitudes on the dayside, near the dawn-dusk terminator at the near-tail flanks, and at high latitudes poleward of the cusp. Coverage of the magnetopause by previous missions has been too limited, however, to support meaningful statistical studies of the global distribution and the morphology of merging sites on the magnetopause or to assess the validity of the various models of magnetopause reconnection that have been proposed. Some of these models predict that sustained reconnection occurs along a line that runs across the magnetopause through the subsolar point and that tilts according to the orientation and magnitude of the magnetosheath magnetic field. Others predict that merging occurs along merging lines in the northern and southern hemispheres, at points where the magnetosheath and terrestrial fields are antiparallel, but not in the subsolar region except in the case of a strictly southward magnetosheath field. Models developed to

explain episodic reconnection invoke reconnection at multiple merging or X-lines or in localized merging patches. Whether reconnection occurs patchily or along single or multiple X-lines may depend in part on the magnetosheath plasma beta (the ratio of plasma pressure to magnetic pressure), a parameter also thought to be important for determining the reconnection rate.

In all dayside reconnection models, the dominant factor that determines where on the magnetopause reconnection occurs is the orientation of the interplanetary magnetic field (IMF) or, in a strict sense, of the magnetosheath field. As the orientation of the magnetosheath field changes, the location of the merging site or sites shifts, moving from lower latitudes for a more southward field to higher latitudes for more northward field. When the IMF is directly northward, reconnection is expected to occur poleward of the cusps; however, it has recently been suggested that, contrary to expectations, weak subsolar merging also occurs for northward IMF. In addition to IMF orientation, other factors thought to influence the location of the merging site (or the tilt of the merging line) include the magnitude of the IMF and the degree to which the Earth's field leaks through the magnetopause and the IMF penetrates into it.

MMS' planned orbit sequence includes both low- and high-inclination magnetopause-skimming orbits. These will make it possible to systematically study the occurrence of reconnection over the entire magnetopause, including the undersampled high latitudes. The location of the merging sites will be established by "triangulation" from simultaneous, spatially separated measurements of plasma flows along the magnetopause. (Changes in the velocity of such tangential flows are a signature of reconnection.) Moreover, through multipoint observations made close enough in time to minimize temporal effects, the MMS cluster will be able to distinguish between patchy reconnection and reconnection occurring along a merging line. With sufficient separation among the spacecraft, MMS will capture the patches; if reconnection is ordered along a line, MMS will identify the line by straddling it.

In addition to measurements of plasma flows within the reconnection layer, concurrent measurements in the magnetosheath by one or two MMS spacecraft will document the local magnetosheath conditions associated with detected reconnection events. These measurements will allow assessment of the influence of factors such as the local magnetic shear and the plasma beta on the merging process and provide a solid observational basis for evaluating different merging hypotheses. For example, observation of subsolar merging at times of low magnetic shear—that is, when the magnetosheath field is predominantly northward—would be evidence for the validity of the component merging hypothesis (as opposed to the antiparallel merging model).

The focus of MMS is on the local, microscale aspects of reconnection. However, from the cumulative local plasma flow and magnetic field measurements, made at different latitudes and different local times, it will be possible to construct statistical

maps showing the global distribution of merging sites on the magnetopause under varying IMF/magnetosheath conditions. **Figure 2.3** suggests what such a global map might look like.

**2.1.2.2 Magnetotail.** Statistical studies show that reconnection occurs in the magnetotail in two regions: at a near-Earth neutral line, in the pre-midnight sector between 20 and 30  $R_E$ ; and at a distant neutral line located at approximately 140  $R_E$  downtail, although sometimes as close in as  $\sim 90 R_E$  (and thus at such times well within the MMS third-phase apogee of 120  $R_E$ ). It is the interplay between the effects of reconnection at these two neutral lines that determines how much of the energy extracted from the solar wind is deposited in the inner magnetosphere and polar ionosphere and how much is channeled down the tail through fast plasma flows and the ejection of plasmoids.

The Geotail mission has provided a wealth of information on both regions, and, in particular, on reconnection and associated phenomena in the near-Earth region. In addition, recent modeling studies—e.g., of current sheet formation or flux rope formation—have advanced our understanding of magnetotail reconnection. However, many questions remain about the nature of reconnection in the tail and about the spatial distribution and morphology of the merging sites. Of particular interest is reconnection in the near-Earth tail and its association with substorms. It is widely recognized that an extremely thin current sheet develops during the substorm growth phase throughout much of the equatorial portion of the near-Earth plasma sheet. Present evidence suggests that this thin current sheet then begins to exhibit localized instability leading to "patchy" magnetic reconnection. It is hypothesized that this reconnection (localized in both azimuth and in radial extent) may give rise to "bursty bulk flows" (BBFs) (see Section 2.3.1.3 below) and sporadic energy dissipation events. What are the spatial and temporal scales for such localized reconnection episodes? How are these patches of reconnection distributed along the length and breadth of the inner portion of the magnetotail? How does this localized reconnection spread to rapidly envelop the whole near-Earth plasma sheet, thereby forming a large-scale plasmoid/flux rope structure?

MMS will address these questions during Phase 2, through measurements in the near-tail reconnection region. Merging at the distant neutral line will be investigated during Phase 3.

### **2.1.3 How Does Reconnection Vary with Time, and What Factors Influence Its Temporal Behavior?**

Reconnection is a time-varying process. The nature of its temporal character, however, is not well-understood. Some magnetopause observations indicate that merging takes place in a sustained or "quasi-steady" fashion, over periods of some tens of minutes. Other data have revealed the frequent occurrence at the magnetopause of an impulsive, quasi-periodic merging mode, the flux transfer event (FTE), with an average period of 8 minutes and an event duration of 1 to 2 minutes (see Section 2.1.4). Further evidence of the variability of reconnection on

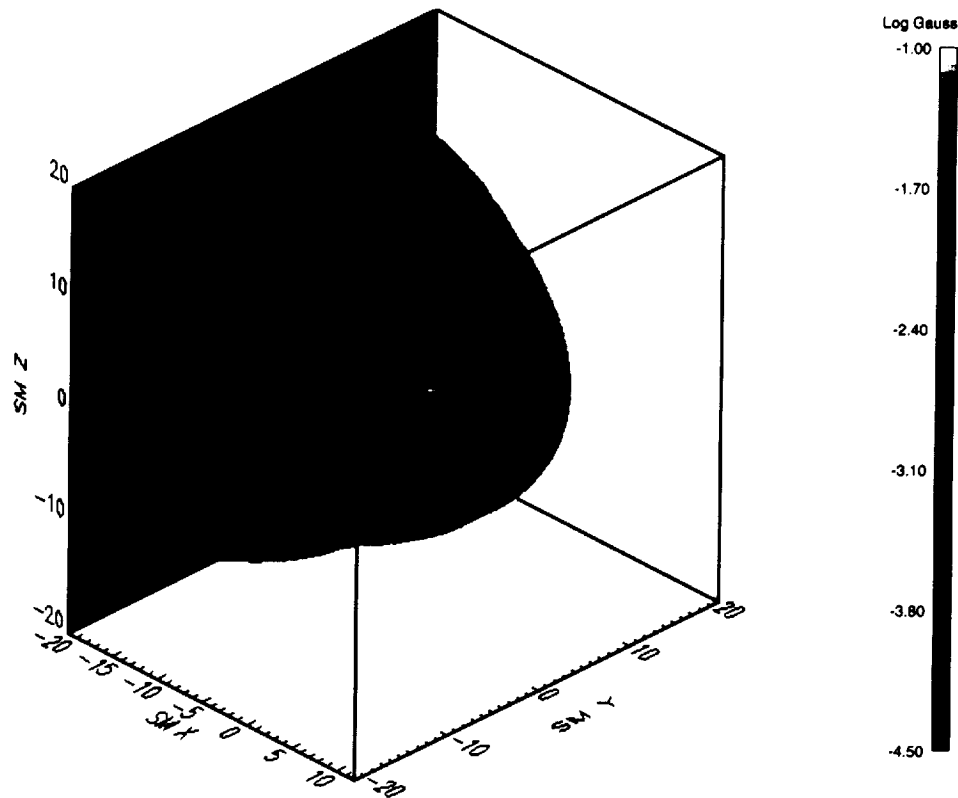


**Figure 2.3.** Computer-generated view of the magnetopause as represented by a surface defined by the Earth's last closed field lines. Red indicates a strong magnetic field, green a weaker field. The view is from above and to the left of the Earth-Sun line. The green feature that can be seen along the high-latitude flanks of the magnetopause (above the equatorial plane on the dusk side, and below it on the dawn side) has been termed the magnetospheric "sash" [White *et al.*, 1998]. It is a region of low magnetic field strength that appears in all global MHD simulations and that is thought to be an active merging site. In these images, the IMF is assumed to lie in the equatorial plane of the geomagnetic dipole. As the IMF orientation changes, so does the orientation of the sash. The mapping of merging sites by MMS as the spacecraft cluster skims along the magnetopause is expected to verify the existence of this predicted feature.

short time scales is provided by steplike discontinuities in the dispersion of precipitating solar wind ions in the cusp. These ion dispersion signatures have been interpreted as evidence for "pulsed" reconnection, resulting from short-term enhancements in the rate of reconnection at the subsolar magnetopause followed by intervals of slower or no reconnection. Recent analysis of Polar data shows that such pulses of enhanced reconnection can last from 0.5 to 3.5 minutes, with 1.2- to 2.9-minute intervals between them. Care must be taken, however, in attributing such dispersion signatures solely to fluctuations in the reconnection rate, as they may also result from the passage of a single spacecraft through a static spatial structure.

In the near-Earth tail, reconnection occurs episodically, in association with the explosive release of energy during the substorm expansion phase. It proceeds initially at a relatively slow rate, with the merging of closed field lines, and then occurs more rapidly as open field lines in the lobe begin to merge. Because of the hypothesized association of bursty bulk flows with reconnection, it has been suggested that near-tail reconnection occurs in a bursty fashion. In the far-tail, on the other hand, reconnection is expected to occur at a slow, steady rate. Recent Geotail data show that it occurs more rapidly near the center of the distant tail than at the flanks.

The **local rate of reconnection** is one of the fundamental parameters that MMS will measure. Theoretical estimates of this rate are in the range of one-tenth of the Alfvén speed. Determination of the reconnection rate through direct measurement will provide a context for the interpretation of MMS' plasma and field measurements in and near the diffusion region and will yield fundamental insights into the processes by which particles are accelerated away from the reconnection region.

To establish the local merging rate, MMS will employ three methods, each of which requires simultaneous measurements from multiple points in space. The first method is to measure the inflow velocity or, equivalently, the dimensions of the diffusion region. Here multipoint measurements are needed to identify the diffusion region and the inflow and outflow regions and to establish their macroscopic motion. The second method is to measure the magnetic field component normal to the magnetopause or magnetotail current sheet, which is a small fraction of the total magnetic field. The third means of determining the reconnection rate is to measure the reconnection electric field, which is the tangential component of the electric field in the vicinity of the X-line. In the case of the last two methods, multipoint measurements allow the boundary orientation to be determined and boundary motion to be cor-

rected for, thus eliminating two difficulties that beset efforts to make these measurements with a single spacecraft.

In addition to measuring the local reconnection rate, MMS will investigate external factors that affect it. For example, statistical studies suggest that the rate of reconnection at the magnetopause is influenced by the magnetosheath plasma beta: when the plasma beta is low, reconnection is more likely to occur, and merging takes place at a faster rate. However, a direct link between this parameter and reconnection at the magnetopause in individual observations has not been established. Measurements by one of the MMS spacecraft in the magnetosheath while the rest of the cluster makes measurements within the reconnection layer will make it possible to assess the influence of the plasma beta on the merging rate. Other environmental factors whose effects on the merging rate MMS will study include the degree of shear between the magnetosheath and terrestrial magnetic fields, the thickness of the current sheet in the near-tail region, and plasma shear flow velocity at the flank magnetopause.

#### 2.1.4 How Are Flux Transfer Events and Plasmoids/Magnetotail Flux Ropes Formed, and How Do They Evolve?

Episodic reconnection has been associated, both at the magnetopause and in the magnetotail, with the formation of magnetic structures characterized by a bipolar signature in the magnetic field component normal to the current sheet. Spacecraft magnetometer data indicate that these structures often contain strong core magnetic fields and twisted field lines, features that are characteristic of magnetic flux ropes (Figure 2.4).

**2.1.4.1 Flux Transfer Events.** The structures observed at the magnetopause are thought to be flux tubes consisting of merged magnetosheath and magnetospheric field lines that propagate tailward across the magnetopause from a merging site near the equator. The plasma within the flux tube consists

of a mixture of magnetosheath and magnetospheric plasmas, and the field within a number of flux tubes is found to have a twisted, flux-rope-like geometry. The formation of such flux tubes and their convection across the surface of the magnetopause is referred to as a “flux transfer event” (FTE). These events occur when the orientation of the IMF is southward or horizontal (but not northward) and have been observed across the dayside magnetopause, from the dawn flank to the dusk flank. It is estimated that they occur approximately 50% of the time under conditions of southward IMF. FTEs are of short duration, lasting 1-2 minutes, and appear to occur quasi-periodically, with an average period of about eight minutes. This quasi-periodic behavior is observed even when the IMF orientation is steady. The cause of the quasi-periodic occurrence of FTEs has not been established. Suggested explanations include variations in the reconnection rate resulting from changes in the orientation or magnitude of the IMF, “rocking” of the merging line by fluctuations in IMF orientation, and the cyclical build-up and release of energy at the magnetopause.

The mechanism responsible for FTE formation has not been identified, although several models have been proposed. The original suggestion was that FTEs were formed at a single reconnection site of narrow longitudinal extent by a process that started and stopped repetitively. The eight-minute repetition was interpreted as the time required to re-initiate merging once it had stopped. A second suggestion is that reconnection takes place at two X-lines and that this pair of X-lines led to the generation of a flux rope. A conjecture similar to the first is that reconnection occurs along a single X-line on the magnetopause, rather than at a point, and that surges in the reconnection rate lead to bubble-like bulges in the reconnected tube. A fourth idea is that reconnection can occur in a patchwork manner on the magnetopause, enhanced by the Kelvin-Helmholtz instability. In addition, solar wind pressure pulses, which produce ripples or waves on the surface of the magnetopause, have been proposed as an alternative to reconnection to explain some of the events identified as FTEs.

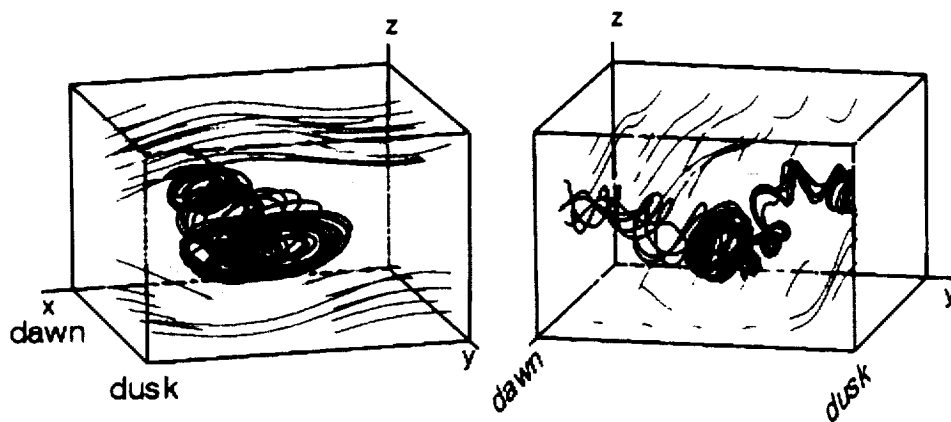


**Figure 2.4.** Two views of a plasmoid, as generated in a 3-D kinetic simulation of magnetic reconnection in the tail [Winglee *et al.*, 1998]. These simulations demonstrate how reconnection can lead to the complex flux rope topology believed to be characteristic of many plasmoids. The five MMS spacecraft, flying in hexahedral formation, will be able to characterize the three-dimensional internal magnetic structure of plasmoids and will investigate the relationship between flux-rope-type plasmoids and “bubble-like” plasmoids.

Assessing the validity of the various mechanisms proposed to account for FTEs has proven difficult because data have been available from at most only two closely spaced satellites and thus have not been sufficient to determine the three-dimensional geometry and motion of these structures. With five spacecraft, however, MMS will be able to determine the geometry of FTEs precisely and to measure their velocities. By probing the size and orientation of FTEs as a function of location on the magnetopause and solar wind/magnetosheath conditions, MMS will be able to identify the source region, generation process, and controlling factors.

**2.1.4.2 Plasmoids/Flux Ropes.** In the magnetotail, the most common products of magnetic reconnection are plasmoids and magnetotail flux ropes. These structures are generated in association with the explosive release of energy during magnetospheric substorms. Plasmoids are large, three-dimensional segments of the plasma sheet that are ejected down the tail at speeds of  $\sim 300\text{--}600\text{ km s}^{-1}$ . Typical volumes are on the order of  $\sim 10^3\text{--}10^4$  cubic Earth radii. These complex structures begin to form in the very early stages of magnetotail activity. Plasmoid ejection begins when the last closed field line in the

plasma sheet merges. Plasmoids rapidly expand in size immediately following their release, and their speed appears to increase as they travel away from the Earth. The causes for this rapid evolution and its relation to the nature of the reconnection process at the near-Earth and distant neutral lines have not been established and will be a focus of the MMS investigation during Phase 2, when apogee is on the night side at  $30 R_E$ , and during Phase 3, when apogee is in the distant tail between  $100 R_E$  and  $120 R_E$  during the transition from low to high orbital inclination.

The internal magnetic structure of the plasmoids has been found to be quite complex and variable: some plasmoids appear to have the expected closed loop topology and a weak field, but many possess a strong core field and have a helical structure consistent with the topology of magnetic flux ropes (**Figure 2.4**). Many questions remain to be answered concerning their three-dimensional structure and connection to the rest of the tail or their evolution with time. In particular, how plasmoids can develop core fields whose magnitude exceeds that of the surrounding lobes remains poorly understood. Theoretical explanations have been developed that propose

Question	<i>What are the kinetic processes responsible for collisionless magnetic reconnection, and how is reconnection initiated?</i>	<i>Where does reconnection occur at the magnetopause and in the tail, and what influences where it occurs?</i>	<i>How does reconnection vary with time, and what factors influence its temporal behavior?</i>	<i>How are FTEs and plasmoids/tail flux ropes formed, and how do they evolve?</i>
<b>Orbit</b>	1.5 x 12 $R_E$ equatorial orbit with dayside apogee (magnetopause study); 1.5 x 30 $R_E$ nightside apogee (tail study) and with 120 $R_E$ nightside apogee during transition to high-inclination orbit (distant tail study); polar orbit skimming the magnetopause from high to low latitudes	1.5 x 12 $R_E$ equatorial orbit with dayside apogee (magnetopause study); 1.5 x 30 $R_E$ nightside apogee (tail study) and with 120 $R_E$ nightside apogee during transition to high-inclination orbit (distant tail); polar orbit skimming the magnetopause from high to low latitudes	1.5 x 12 $R_E$ equatorial orbit with dayside apogee (magnetopause study); 1.5 x 30 $R_E$ nightside apogee (tail study) and with 120 $R_E$ nightside apogee during transition to high-inclination orbit (distant tail); polar orbit skimming the magnetopause from high to low latitudes	Polar orbit skimming the magnetopause from high to low latitudes (FTE study); 1.5 x 30 $R_E$ nightside apogee and 120 $R_E$ nightside apogee during transition from low- to high-inclination orbit (plasmoid/flux rope study)
<b>Spacecraft Separation</b>	10 km to 1 $R_E$	0.25 to 2 $R_E$	10 km to 1000 km	50 to 500 km (FTE study); 1000-25,000 km (plasmoid/flux rope study)
<b>Measured Parameters</b>	<ul style="list-style-type: none"> <li>· Magnetic field</li> <li>· Reconnection Electric field</li> <li>· Current densities</li> <li>· Dimensions of diffusion region</li> <li>· Inflow and outflow ion and electron velocities</li> <li>· Electron Pressure Anisotropies</li> </ul>	<ul style="list-style-type: none"> <li>· Magnetic field</li> <li>· Plasma flow velocities</li> <li>· Electric field parallel to the magnetic field</li> </ul>	<ul style="list-style-type: none"> <li>· Magnetic field normal to magnetopause</li> <li>· Reconnection electric field</li> <li>· deHoffman-Teller velocity</li> <li>· Dimensions of diffusion region</li> <li>· Inflow and outflow ion velocities</li> </ul>	<ul style="list-style-type: none"> <li>· Magnetic field</li> <li>· Plasma density, velocity, and composition</li> <li>· Electron and ion 3-D distribution functions</li> <li>· Electromagnetic and electrostatic components of plasma waves</li> <li>· Energetic particles</li> <li>· Electric field</li> </ul>

**Table 2.2.** Measurement requirements for the MMS reconnection investigations.

either a “collapse” of the plasmoid core as hot plasma is lost as a result of the connection of plasmoid field lines to the much cooler magnetosheath or an amplification of the pre-existing plasma sheet  $B_y$  field. Another possibility is that the reconnection process itself generates, at times, more bubble-like plasmoids, and at other times, helical flux rope structures. Other possibilities such as the non-linear amplification of MHD waves in the current sheet have also been proposed.

The MMS mission design calls for the MMS spacecraft cluster to dwell in the near tail at  $\sim 30 R_E$  during the second phase of the mission and to traverse the distant tail at  $\sim 120 R_E$  during the third phase. Thus MMS will be able both to investigate plasmoid/flux rope formation in the near-Earth reconnection region and to learn how these structures evolve as they move tailward. Through multipoint magnetic field and plasma measurements, MMS will determine the dimensions, magnetic topology, and stress balance of the plasmoids/flux ropes. Separations as small as 1000 km will be required to examine the high field core region of the flux ropes, while separations of at least 25,000 km will be necessary to determine the larger-scale dimensions of the flux ropes/plasmoids and to study their interaction with the surrounding magnetotail.

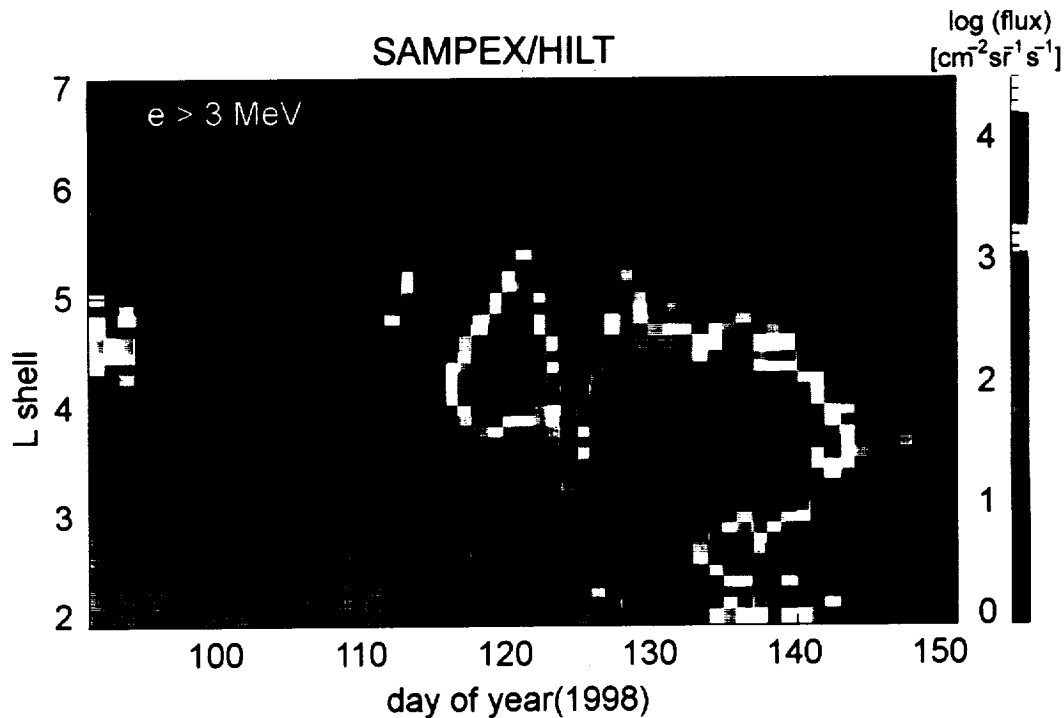
### 2.1.5 Experimental Requirements for the MMS Reconnection Investigation

Table 2.2 on the previous page, summarizes the measurement parameters and recommended interspacecraft distances for

each of the four key science questions that constitute the MMS reconnection investigation. The orbital phases during which each question will be addressed are also indicated.

## 2.2 Particle Acceleration

Energy is transferred from the solar wind into the Earth’s magnetosphere through several processes, including magnetic reconnection at the dayside magnetopause and shear-generated turbulence along the magnetopause. Initially, much of this energy goes into large-scale current systems inside the magnetosphere; it is then, over periods of minutes to hours, redistributed. An important byproduct of this process is the acceleration of charged particles to high-energies. As a result, electrons, protons, and heavy ions are found throughout the magnetosphere with energies up to many thousands of eV and even many millions of eV and are typically described by a power law distribution. In the inner magnetosphere, the accelerated particles are trapped in the Earth’s magnetic field, forming the ring current and the radiation belts (Figure 2.5). Traditionally, the trapped particles have received the most attention with regard to the physics of energetic particles. In the outer magnetosphere, accelerated populations are more highly time-dependent. Yet everywhere the energized particles play an important role in the transfer of energy from currents and fields into the plasma, and in the transport of energy from the initial acceleration region to other parts of the magnetosphere and beyond. It is also known that high-energy particles represent a



**Figure 2.5.** Enhancements of highly relativistic (>3 MeV) electrons in the Earth’s radiation belts observed with the SAMPEX Heavy Ion Large Telescope (HILT) during a period of intense solar and geomagnetic activity in April and May of 1998. Beginning on day 124, when the Dst dropped to -218 nT and the solar wind speed reached a high of  $\sim 850 \text{ km s}^{-1}$ , intense relativistic electron fluxes appeared deep in the magnetosphere, at altitudes below  $L \sim 3$ , and a new radiation belt formed at  $L \sim 2.2$  [Baker et al., 1998]. MMS will investigate the acceleration mechanisms responsible for such dramatic enhancements.

serious natural hazard for satellites operating in certain portions of the geospace environment: their extreme energies can lead to deep dielectric charging of sensitive electronic parts and to intrinsic damage of microelectronics through ionizing radiation.

Charged particles are accelerated by the forces exerted on them by electric fields. In the magnetosphere, several acceleration mechanisms are at work. Each combines a different set of magnetic and electric configurations and time dependences to accelerate particles in ways characteristic of that particular mechanism. The principal mechanisms are Fermi acceleration, betatron acceleration, wave-particle interactions, inductive electric fields, and parallel electric fields. (Shocks also accelerate particles; however, shock acceleration processes are really special cases of the various mechanisms just listed.)

MMS is ideally suited to advancing our knowledge and understanding of how acceleration mechanisms operate in the magnetosphere. Specifically, MMS will directly measure the inductive electric field and the gradients in  $\mathbf{B}$  and  $\mathbf{E}$  and will remove the time/space ambiguity inherent in single spacecraft measurements. It will provide excellent determination of the mesoscale configurations of electric and magnetic fields in and near the thin current sheet regions at boundaries. In addition, owing to high-speed motion, energetic particles act as effective tracers of remote acceleration processes: the energetic particle sensors on the five MMS spacecraft will provide a powerful diagnostic for remotely sensing the boundary structure (i.e., through the use of finite gyroradius “sounding”) as well as for identifying the acceleration processes that occur within these boundaries (i.e., through the use of phase space density features produced through reconnection). These data will complement the hexahedral magnetic and electric field sensors that provide the gross electromagnetic topologies. Concurrently measured electromagnetic wave data will allow us also to test theories that invoke free energies within the plasma to diffusively or resonantly accelerate particles.

### **2.2.1 What Is the Role of Inductive Electric Fields and Wave-Particle Interactions in High-Energy Particle Acceleration?**

In-situ observations have clearly demonstrated the abrupt appearance within the magnetosphere of multi-MeV electrons and ions. The absolute intensities of these particle fluxes can be extremely high, and studies of phase space density profiles clearly establish that these very energetic particles have not merely been shifted around in a spatial sense. Rather, these observations strongly imply that the Earth’s magnetosphere functions as a powerful, efficient particle accelerator in its own right (see **Figure 2.5**). Both inductive electric fields and wave-particle interactions operate in the magnetosphere to accelerate magnetospheric charged particles rapidly to extremely high energies.

**2.2.1.1 Inductive Electric Fields.** In considering possible acceleration mechanisms, it is evident that the electric fields

responsible for multi-MeV ions and electrons cannot be field-aligned potential drops nor can they be large-scale electrostatic fields. A “single-step” electric field interaction would require either that potential drops be enormous (much higher than are observed in space) or else that they extend over scale sizes much larger than the entire magnetosphere. Thus, observations of high-energy ion pulses during magnetospheric substorms and of relativistic electron enhancements during geomagnetic storms require that acceleration occur through the action of inductive electric fields. Stated differently, rapidly changing magnetic fields in key regions of geospace produce the highest energy magnetospheric particles.

In order to study very energetic particle acceleration and the localized, highly fluctuating magnetic fields that produce such particle events, it is necessary to characterize the temporal and spatial scales of the field changes. The MMS mission—with its complement of particles and fields sensors—is ideal for attacking the problem of inductive electric field acceleration. During major geomagnetic storms and related powerful particle acceleration events, it will be possible to examine the low-frequency magnetic fluctuations as well as the rapid magnetic reconfigurations that constitute strong inductive electric field events. The MMS energetic particle detectors will allow detailed spectral and spatial comparisons with present theoretical models.

**2.2.1.2 Wave-Particle Interactions.** Charged particle acceleration also results from resonant interactions with wave fields. This interaction produces a non-thermal shape to an otherwise thermal distribution. In magnetospheric plasmas, there exists a rich spectrum of naturally occurring plasma waves as well as a host of magnetohydrodynamic (MHD) waves. These waves span scale sizes as small as electron inertial lengths (<10 km) and as large as MHD-scale waves standing on magnetospheric field lines (many Earth radii). These waves may be global, regional, or quite localized. The characteristic time scales range from fractions of a second to several tens of minutes. To extract and gain energy from the wave electric fields, accelerated particles must have a net, time-averaged resonance with the wave fields. Each wave mode can potentially accelerate different components of the population.

Recent evidence from the International Solar-Terrestrial Physics (ISTP) program confirms that non-thermal particles may be accelerated very efficiently through wave-particle interactions. For example, in the inner magnetosphere, observations of a rapid increase in >1 MeV electrons during magnetic storms have been linked to increases in global ultra-low-frequency MHD waves. These waves intensify when a bursty solar wind buffets the magnetosphere, exciting internal cavity modes. Theoretical modeling has shown that such waves can indeed energize particles that are in net drift resonance with these global modes. Based on these observations, there is compelling reason to believe that this same sort of mechanism might be operative elsewhere in the magnetosphere on a more modest spatial scale and for more typical geomagnetic conditions.

MMS will provide the requisite wave measurements to address the issues of particle acceleration through wave-particle interactions. In the first two phases of the mission, the MMS spacecraft will traverse the inner magnetosphere with separations ranging from hundreds of kilometers to approximately an Earth radius. Wave measurements in this region will permit assessment of the localization of key wave modes and their spatial and temporal coherence. Coincident energetic particle measurements will be used to test models of proposed wave-particle interaction mechanisms such as drift resonance.

### **2.2.2 How Are Particles Accelerated in Plasma Injection Events in the Near-Earth Tail?**

During the course of explosive energy conversion events (at the onset of magnetospheric substorms), there are often observed powerful, extremely impulsive high-energy ion and electron “injection” events. These have been observed most extensively near geostationary orbit ( $6.6 R_E$  geocentric distance) within the middle magnetosphere. A dramatic example of such an event is shown in **Figure 2.6**. The initial particle injection pulse is temporally narrow ( $<1$  min in duration), extends to very high energies ( $>1$  MeV), and represents a flux increase of several orders of magnitude over the background flux (in the energy range of 100-1000 keV). Once the particle pulse appears in the middle magnetosphere, it is entrained on magnetic field lines, and the particle population drifts rapidly around the Earth under the influence of the magnetic gradient and curvature forces to form a “drift echo” event.

How are such brief, powerful acceleration events possible? Are they similar to impulsive particle acceleration events on the Sun and in other planetary environments (e.g., Mercury, Jupiter, Saturn)? Such questions have been asked for many years, but the means have not been available to address the key issues in such plasma injection events: Where do the “seed” particles originate that form the injected population? What combination of inductive and non-inductive electric fields accelerates the particles to such high energies on such short time scales? What pathway do particles follow in order to ultimately form such a narrow spatial and temporal pulse? And, what is the energy spectrum and “efficiency” of the injection/acceleration process?

Fermi acceleration is a likely candidate for particles in the nightside magnetosphere. Particles distributed along magnetic field lines are confined to the magnetospheric region by the magnetic mirror effect associated with the strong magnetic field increase near the Earth. During the dynamical evolution of the nightside magnetosphere, energy loading generates strongly stretched magnetic field lines whose equatorial legs are extended far in the antisunward direction. The antisunward displacement of the stretched field lines in the plane of the magnetic equator can be as large as several Earth radii. The rapid dynamical evolution of the substorm abruptly changes this stretched configuration in a process known as “dipolarization.” Dipolarization generates a rapid convective earthward

motion and shortening of the stretched field lines. The resulting magnetic field resembles, in magnitude and flux tube shape, the unperturbed dipole magnetic field of the Earth.

The substantial shortening of magnetic flux tubes likely has a profound effect on the resident plasma particle population. The dynamical shortening of magnetic flux tubes, together with the effective trapping of particles by mirror forces, leads to a Fermi-type acceleration process, which primarily affects the energy of particles parallel to the magnetic field. In addition to this effect, a competing process, betatron acceleration resulting from the magnetic field increase during dipolarization, leads to a perpendicular energy increase. The competition between these two processes is regulated by the equatorial dwell-time of charged particles (longer times favoring stronger betatron acceleration), and the amount of flux tube shortening, which favors Fermi acceleration.

The relative importance of these two processes remains an open question, but one that will be answered very effectively by the MMS mission. The spacecraft cluster provides an opportunity to study the evolution of parallel and perpendicular energies of particles on flux tubes moving across the configuration. Together with magnetic field and inductive electric field measurements, a direct assessment of the relevance of both of these effects is readily feasible by energetic particle measurements.

### **2.2.3 What Are the Mechanisms for Accelerating Charged Particles at Plasma Boundaries?**

The ongoing ISTP project has explored not only the better-studied energetic particle regions of the inner magnetosphere, but also the appearance of energetic particles in other regions of geospace, including distant boundary layers. These studies have revealed the often global nature of magnetospheric acceleration processes and have underscored the critical importance of accurately knowing the seed populations located in the weaker magnetic field regions. As an example, ISTP measurements have identified a heretofore unmeasured population of very energetic ions and electrons in the high-altitude magnetospheric cusp. These observations reveal large fluxes of non-thermal charged particles, co-located in regions of very weak magnetic fields and extremely intense plasma waves. Several mechanisms have been proposed to explain these observations. Two of the mechanisms invoke distant acceleration (e.g., upstream of the quasi-parallel shock) and then subsequent access of these particles into the outer cusp region. One of the models, however, proposes that the particles are accelerated in situ by wave turbulence in the natural trapping geometry of the cusp. The exact role of these various mechanisms remains unclear. Whatever the specific acceleration process, this population appears to be a robust feature of the cusp and thus potentially of the entire magnetopause boundary layer. As such, it may well represent an important boundary condition for describing energetic particle populations inside the magnetosphere.

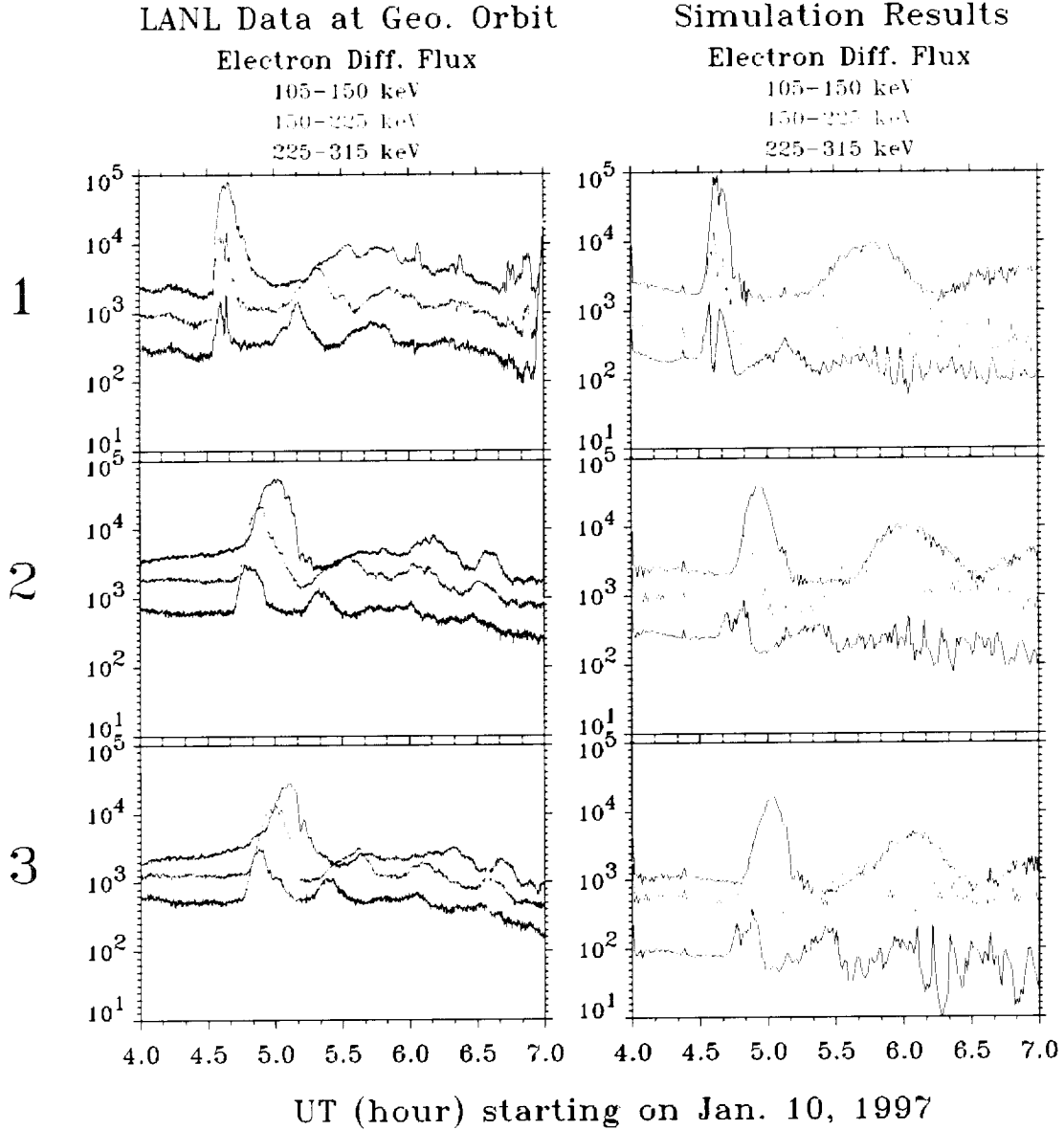


**Figure 2.6.** The three panels on the left show the signatures of an energetic electron injection event detected in three different energy ranges by three geosynchronous satellites separated in local time. The peak flux enhancement is observed by the first satellite at ~04:40 UT and at progressively later times by the second and third satellites as the electrons gradient-drift eastward around the Earth. As the electrons continue to drift around the Earth, they are detected again by the satellites, producing smaller peaks in the data known as “drift echoes.” The panels on the right show the results of a test-particle simulation that successfully reproduces the observed features. The model results indicate that such injection events can result from betatron acceleration by transient electric and magnetic fields associated with substorm dipolarization [Li *et al.*, 1998].

In the final mission phase, when the five spacecraft are traversing the high-latitude magnetopause, MMS will be able to solve the mystery of the energetic cusp population. The orbit will provide latitudinal cuts through the outer cusp region, potentially with the spacecraft straddling the magnetopause. Such configurations will provide coincident measurements of the wave properties in the magnetosphere, in the magnetosheath, and in the cusp at the same time that the energetic tail of the particle distributions is also being measured. Such measurements should definitively determine whether the energetic cusp particles are accelerated remotely or locally through waves.

Like the magnetopause, the magnetotail current sheet is often very thin compared to the energetic particle gyroradius. Non-MHD, microphysical effects are thus likely to be important near such thin boundary regions. At these boundaries, particles become “non-magnetic” and may feel the accelerating effects of large electrostatic potentials that are approximately perpendicular to the magnetic field lines. Indeed, hints of this behavior are seen in some data that remotely sense thin current regions. Theoretical predictions of features in phase space density of energetic particles produced within thin current sheets have been put forth with various levels of sophistication from numerical modeling approaches. However, in reality, space-time ambiguities of the magnetic and electric field structure often confound a straightforward interpretation of such observations in the context of such models. MMS will be ideal for addressing the acceleration of particles at thin boundaries.

Electric fields exhibiting a significant magnetic field-aligned component are natural acceleration mechanisms for charged particles. Parallel electric fields are an essential ingredient in the magnetic reconnection process, particularly at the magnetopause, but also in the magnetotail. It has been shown that the maximum value of the integral of  $E_{\parallel}$  along magnetic field lines is equal to the rate of magnetic flux reconnection. For the magnetotail, modeling has shown that energies obtained this way can range up to some 100 keV for average flux reconnection rates associated with magnetotail dynamics. Observations both at the magnetopause and in the magnetotail indicate, on the other hand, that reconnection processes are often bursty, involving the rapid reconnection of large amounts of magnetic flux, such as is associated, for example, with bursty bulk flows (BBF). For these very large reconnection rates even higher energies may result. Acceleration by parallel electric fields is thought to be important in other astrophysical systems (e.g., extragalactic jets and pulsar magnetospheres) as well as in the terrestrial magnetosphere. It is therefore important to further investigate regions of parallel electric fields and study their viability as particle acceleration mechanisms at both day- and nightside magnetosphere.

With its combination of electric and magnetic field instruments and energetic particle and thermal plasma detectors, the five MMS spacecraft will be able to probe the structure of parallel electric fields and obtain the data needed to assess their efficiency as particle acceleration mechanisms. These studies, along with others involving, for example, inductive electric

fields, will make it possible to evaluate the relative importance of individual acceleration processes in different magnetospheric regions as well as to determine their role as overall providers of the magnetospheric energetic particle population.

#### **2.2.4 Experimental Requirements for the MMS Particle Acceleration Investigation**

**Table 2.3** summarizes the measurement parameters and recommended interspacecraft distances for each of the three key science questions that constitute the MMS particle acceleration investigation. The orbital phases during which each questions will be addressed are also indicated.

### **2.3 Turbulence**

Turbulence is ubiquitous in the solar wind-magnetosphere system and indeed throughout the universe. In a broad sense, turbulence refers to coupled nonlinear fluctuations spanning a wide range of spatial and temporal scales in the plasma. At the largest scales, the phenomena can be described by MHD (or fluid) turbulence, which bears resemblance to the behavior of the more familiar geophysical and atmospheric turbulence. At smaller and smaller scales, electromagnetic interactions and plasma instabilities assert themselves and produce microturbulence phenomena that are unique to space plasmas. The intrinsic importance of understanding the nature of turbulence in nonuniform plasmas, together with this multiscale property, makes it a natural and compelling scientific target for the MMS mission.

The study of fluid turbulence in space plasmas has been brought to its conceptually most advanced stages in the solar wind. However, in the boundary regions to be sampled by the MMS spacecraft, use of some of the concepts and assumptions appropriate for the study of solar wind turbulence is not justified a priori. In qualitative terms, the difference between turbulence in these regions and turbulence in the solar wind is somewhat akin to the difference between ordinary fluid mechanical turbulence in a viscous shear layer and turbulence behind wire grids. The latter type can be considered homogeneous and isotropic while the former is driven by macroscopic velocity shear and has rather different properties, including the possibility of inverse cascades in 2-D systems, i.e., cascades to larger rather than smaller scale sizes and resulting self organization. Nevertheless, quantities such as the average velocity distribution in a shear layer and the turbulent eddy viscosity exhibit universal scaling and highly reproducible behavior. In the layers to be probed by MMS, measurements from five spacecraft are essential in order to provide the necessary statistical characterization of spatial and temporal features of the turbulence, identify underlying physical processes, and derive scaling laws that permit use of MMS results in contexts other than Earth’s magnetosphere.

The following discussion is organized according to questions applicable to the different boundary regions of the magnetosphere because of the unique conditions that exist in each of

Question	<i>What is the Role of Inductive Electric Fields and Wave-Particle Interactions in High-Energy Particle Acceleration?</i>	<i>How are Particles Accelerated in Plasma Injection Events in the Near-Earth Tail?</i>	<i>What are the Mechanisms for Acceleration of Charged Particles at Plasma Boundaries?</i>
<b>Orbit</b>	<ul style="list-style-type: none"> <li>• 1.5 x 12 R<sub>E</sub> equatorial orbit with nightside apogee</li> <li>• 1.5 x 30 R<sub>E</sub> equatorial orbit with nightside apogee</li> </ul>	<ul style="list-style-type: none"> <li>• 1.5 x 12 R<sub>E</sub> equatorial orbit with nightside apogee</li> </ul>	<ul style="list-style-type: none"> <li>• 1.5 x 12 R<sub>E</sub> equatorial orbit with dayside apogee</li> <li>• 1.5 x 12 to 30 R<sub>E</sub> apogee raising equatorial transition orbit</li> <li>• Polar orbit skimming the magnetopause from high to low latitudes</li> </ul>
<b>Spacecraft Separation</b>	100 km to 1 R <sub>E</sub>	100 km to 1000 km	10 km to 1000 km
<b>Measured Parameters</b>	<ul style="list-style-type: none"> <li>• <math>d\mathbf{B}/dt</math></li> <li>• <math>\nabla \times \mathbf{E}</math></li> <li>• EM wave spectra</li> <li>• 3-D electron and ion phase space density of plasma and non-thermal tail of distribution</li> <li>• Anisotropies</li> </ul>	<ul style="list-style-type: none"> <li>• EM wave spectra</li> <li>• 3-D electron and ion phase space density of energetic particles with energies from 100 keV to 1000 keV</li> </ul>	<ul style="list-style-type: none"> <li>• 3-D magnetic and electric fields within boundary layers</li> <li>• EM wave spectra</li> <li>• 3-D electron and ion phase space density of plasma and non-thermal tail of distribution</li> </ul>

**Table 2.3.** The measurement requirements for the MMS particle acceleration investigation.

them. Taken as a whole, the range of fluid and microturbulent phenomena and the coupling to reconnection and particle acceleration that is expected to be encountered in these regions enable in effect a comprehensive laboratory study of turbulence with results that can be generalized to other astrophysical environments.

### **2.3.1 What Are the Temporal and Spatial Properties of, and the Physical Processes Responsible for, Turbulence in the Magnetosheath, Magnetopause, and Plasma Sheet?**

**2.3.1.1 Magnetosheath Turbulence.** The magnetosheath, the transition region between the bow shock and the magnetopause, is the site of turbulence from various sources. For example, solar-wind turbulent structures convect across the bow shock into the magnetosheath; fluctuations generated at the bow shock (in particular in regions where it has quasiparallel geometry) propagate downstream into the magnetosheath; fluctuations generated by Kelvin-Helmholtz or Rayleigh-Taylor instabilities at the magnetopause propagate upstream into the magnetosheath; and local instabilities, in particular mirror and ion cyclotron modes, which are driven by anisotropy in particle distribution functions within the magnetosheath, occur on the meso and microscales. For lack of mul-

tispacecraft data, the roles played by these various sources, and their relative importance in determining the properties of magnetosheath turbulence, remain largely unexplored. The MMS mission will be optimally configured to address these issues.

An important example of mesoscale magnetosheath turbulence, especially near the magnetopause, is the magnetic mirror mode. The mirror mode is an important object of study because it appears to be a common phenomenon in solar system plasmas. It has been observed in the solar wind, in the magnetosheaths of outer planets, in the wake of Io, and in the coma of comets. Like the ion cyclotron instability, it is driven by thermal pressure anisotropy, in which the pressure perpendicular to the magnetic field exceeds that along the field. It creates spatial structure in the form of alternating regions of high plasma pressure accompanied by low magnetic field pressure and low plasma pressure accompanied by high field pressure.

Determining the reason for the appearance of mirror mode waves in these plasmas is a two-fold problem. We need to understand the mirror mode waves themselves, their geometrical properties (e.g., sheet-like or tube-like), scale sizes and intensities, and the conditions under which they arise. We also need to understand why the ion cyclotron instability, which grows from the same pressure anisotropy and which, judging

from numerical simulations, appears to be an effective agent in limiting the magnitude of the anisotropy, does not succeed in quenching the mirror mode. Possible explanations include ion compositional effects that destroy the cyclotron resonance and spatial inhomogeneities that spoil the coherence of the cyclotron motion of the resonant ions. Measurements of ion composition and spatial gradients are therefore essential to the study of mirror mode waves. The lack of such measurements on previous missions in which mirror mode waves were found has been a serious impediment to progress.

The MMS Mission can enhance our understanding of mirror mode waves by exploring those waves that occur in the magnetosheath near the magnetopause. The transverse scale size of the wave-generated structures is believed to be several gyro-radii, of the order of 200 km. The separation of the spacecraft needed to resolve the geometry is a fraction of this scale, i.e., ideally about 10-50 km. At least four measurements, or three baselines, are needed to determine orientation, aspect ratio, and velocity of the structures.

**2.3.1.2 Magnetopause and Boundary Layer Turbulence.** It is the magnetopause current layer with its adjoining, interior low-latitude boundary layer (LLBL) and exterior plasma depletion layer that is most similar to a turbulent fluid mechanical shear layer, although its behavior is strongly modified and controlled by the magnetic field.

Nonpropagating mesoscale instabilities that may operate in the subsolar magnetopause region and then be transported along the magnetopause in a purely convective manner have not been the subject of extensive observational studies to date. Included here is the Rayleigh-Taylor instability, which may be excited when the magnetopause is caused to accelerate, and the tearing mode, which is discussed later in this section.

All of these wave and instability modes are excellent topics for observational studies with MMS. They are relevant to turbulence because in their nonlinear stages they may develop increasingly short spatial scales and fluctuations that have the basic stochastic nature characterizing turbulence. An important aspect of turbulence is its ability to produce transport. The specific advantage of MMS in this context will be its ability to resolve short spatial and rapid temporal scales to provide quantitative characterization of the turbulence and of its resulting transport.

**Figure 2.7** shows a spatially low-pass filtered map of the magnetopause magnetic field, constructed by integration of the magnetohydrostatic Grad-Shafranov equation, in which magnetic-field and plasma data from a single-spacecraft (AMPTE/IRM) were used as spatial initial conditions. Several tearing-mode islands, separated by X-type null points, are seen in the current layer. These structures convect past the observing spacecraft at a velocity (the deHoffmann-Teller velocity) that can be determined directly from measured plasma velocities and magnetic fields. This figure illustrates one type of mesoscale turbulent tearing-mode structure that may exist in the magnetopause. It also illustrates the extreme anisotropy of such turbulence. The presence of such island structures allows for effective plasma transport from the magnetosheath edge to the magnetospheric edge of the magnetopause layer but not for transport onto geomagnetic field lines. However, it is likely that some of the X points separating the islands serve as seed locations for bursts of patchy reconnection, a process that can provide direct access of magnetosheath plasma to open magnetospheric field lines connected to the ionosphere. A desirable adjunct to MMS is the development of a general field-map reconstruction method, based on the MHD equations, that permits the assimilation of data from several spacecraft to produce field maps at high spatial resolution, describing three-dimensional features and time dependence.

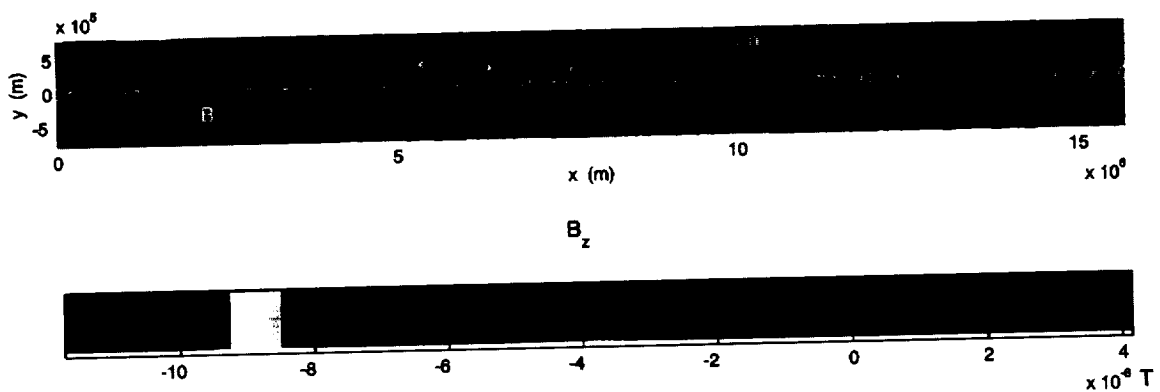


**Figure 2.7.** Map of the magnetopause current layer showing several tearing-mode islands separated by X-type null points. The Z component of the magnetic field is shown in color; as indicated by the color bar, it is positive outside, but negative within the current layer. Yellow circles indicate locations where the data used to construct the map were taken, with the spacecraft moving from left to right. At each circle, the measured transverse field vector is shown. Also shown is the vector  $\mathbf{n}$  normal to the magnetopause, as determined by minimum variance analysis of the measured field. The map is based on magnetic field and plasma measurements by the spacecraft AMPTE/IRM during an encounter with the magnetopause on October 19, 1984 [Hau and Sonnerup, 1999].

**2.3.1.3 Plasma Sheet Turbulence.** Evidence for the presence of vortical flows in the near-Earth equatorial tail region was reported a number of years ago but the prevalence and properties of such wake-like flow phenomena have not been assessed. More recently, events known as current disruptions and bursty bulk flows (BBFs) have been extensively documented as occurring in the geotail environment. They are observed in association with large magnetic field fluctuations and appear to have stochastic properties that allow them to be described as turbulence. Past analyses suggest that they are spatially localized features associated with Earthward transport of significant amounts of particle mass, energy, and magnetic flux. However, uncertainties exist in these results because an accurate assessment of transport produced by BBFs relies on knowledge of their spatial dimensions as well as of their spatial and temporal occurrence patterns. Such knowledge in turn depends on the ability to differentiate between temporal evolution and spatial variation in measured time series, which is difficult or impossible to achieve on the basis of single-spacecraft information. The MMS mission will provide a unique opportunity to separate spatial variation from temporal evolution and to evaluate the role played by turbulence associated with BBFs in producing Earthward transport of particle mass, momentum, and energy, as well as magnetic flux in the magnetotail. Similarly, the importance of cross-tail plasma transport associated with wake-like vortical flows can be quantified.

While these and other observational results indicate the importance of turbulence in the plasma sheet, the basic properties of that turbulence, i.e., quantities such as fluctuation spectrum in the spatial domain, correlation time, correlation length, and mixing length have yet to be determined systematically, a task that requires coordinated multipoint measurements. The MMS mission can be configured to permit determination of these basic parameters of plasma sheet turbulence. A particularly favorable arrangement for some of the geotail studies is to have the individual satellites placed along an equatorial orbit like beads on a string, as they traverse the tail plasma sheet.

### **2.3.2 What Are the Sources, Propagation, and Consequences of Mesoscale Boundary Waves?**

Mesoscale surface waves have been observed from time to time at various locations on the magnetopause with its adjoining low-latitude plasma boundary layer (LLBL). Typical observational characteristics of such wave trains are multiple crossings of the current layer, for which the normal vector  $\mathbf{n}$ , determined for example by minimum variance analysis of single spacecraft magnetic field data, tilts back and forth from one crossing to the next. Wavelengths and propagation directions can be established from single spacecraft information only by the introduction of additional assumptions. At the inner edge of the LLBL, surface waves manifest themselves as the repeated appearance and disappearance of magnetosheath-like plasma at the observing spacecraft. Sometimes measurable flow vector deflections and magnetic field deformations can be seen as well. In addition to wave trains, various solitary structures are also observed to move along the magnetopause. Included here are FTE flux tubes, localized bumps or depressions on the

magnetopause layer, and step-like changes in magnetopause location.

A principal physical mechanism expected to operate in the magnetopause/LLBL region is the Kelvin-Helmholtz instability, which is driven by free energy associated with the velocity shear across the region. Wave growth at mesoscale wave lengths is modest; the resulting expectation is that wave trains have to travel substantial distances tailward from their point of generation before they reach amplitudes where nonlinear effects become important. For this reason, it is important that the proposed MMS orbit phases permit observation of flank and high-latitude magnetopause behavior in the near-Earth tail as well as in the mid-tail and distant-tail regions.

The Kelvin-Helmholtz instability is impeded by shear in the magnetic field that is usually present within the magnetopause current layer; large-amplitude waves on this layer are therefore expected predominantly when and where the local magnetosheath field is parallel or antiparallel to the local geomagnetic field. At the inner edge of the LLBL, the fields on the two sides of the edge are more or less parallel, the result being that Kelvin-Helmholtz wave activity there may be far more common than at the magnetopause. Ordinary MHD analysis of Kelvin-Helmholtz instability on a thin discontinuity indicates that growth rate increases with decreasing wave length. In reality the magnetopause has a thickness of the order of 500 km so that one might expect maximum growth at wavelengths of the order of this thickness. The existence and role of such relatively short surface waves is best explored by multispacecraft missions, such as MMS, that permit small-scale characterization of the waves, including their actual wavelengths and propagation directions.

Even under conditions where the Kelvin-Helmholtz instability cannot operate, stable surface wave motion, initiated by some external disturbance, is possible. Among possible sources for such stable waves and solitons are pressure pulses and other structures, including various plasma discontinuities such as hot-flow anomalies in the magnetosheath, which impinge on the magnetopause.

The nonlinear evolution, interaction, and turbulent transport coefficients pertaining to macroscopic modes, such as the Kelvin-Helmholtz and tearing instabilities, have been studied extensively, both analytically and by use of numerical simulation tools. To date, the many types of behavior predicted from such studies, (e.g., wave breaking and, under some conditions, the occurrence of inverse turbulent cascades and resulting self-organization in the form of vortex or magnetic-island coalescence, have not been verified in spacecraft data for lack of suitable), coordinated multispacecraft information. Similarly, it has not been possible to derive turbulent transport coefficients from the data for comparison with theoretical predictions. With suitable choices of spacecraft separations and cluster configuration, MMS will be ideally configured to bridge these gaps between theory and actual observations of nonlinear phenomena and transport in the magnetopause and its boundary layers.

An ideal MMS mission configuration for studies of mesoscale magnetopause structures would consist of five spacecraft, four of which define a tetrahedron with sides smaller than a typical magnetic island width or Kelvin-Helmholtz wavelength. These four spacecraft serve to establish magnetopause orientation and velocity with high accuracy and to investigate temporal coherence, lateral dimensions, motion and other features of turbulent structures within the magnetopause current layer or of deformations moving along it, such as FTEs or surface waves. The fifth spacecraft should be placed a comparable distance outside the tetrahedron. This spacecraft will help determine the acceleration of the boundary, define spatial properties of turbulence in the direction normal to the magnetopause, and establish plasma and field conditions as well as temporal changes in the magnetosheath during magnetopause encounters by the other spacecraft. The mission configuration described here would also be well suited for studies of certain mesoscale magnetosheath structures. But small spacecraft separations are needed for other studies, (e.g., for the determination of local gradients and current densities), both in the magnetosheath and the magnetopause.

The magnetopause sometimes moves only slowly in the inward or outward direction. Such was the case during the event shown in the field-map shown in Figure 2.7. But more often it exhibits rapid, rapidly changing, and inward/outward motion. Speeds up to  $100 \text{ km s}^{-1}$  or more are not uncommon. For typical magnetopause widths—of the order of  $500 \text{ km}$ —such high speeds lead to observation times of magnetopause structures of only a few seconds. The high time resolution required to study magnetopause structure in such cases is easily achieved by magnetometers and electric probes but poses a design challenge for plasma instruments, for which a data rate of better than one sample per second would be desirable, if the fastest moving magnetopause layers are to be resolved.

### **2.3.3 What Is the Role of Turbulence in Plasma Entry through the Magnetopause?**

The transport of plasma from the magnetosheath, across the magnetopause, and into the magnetosphere is one of the most important physical processes in magnetospheric physics. As discussed in Section 2.1 above, there is conclusive observational evidence that reconnection plays an important role in such transport. However, it has not been firmly established whether, —and in what circumstances, —reconnection operates as a predictable and geometrically well-organized global process or sometimes qualifies as turbulence by occurring in a small-scale stochastic manner. The latter situation has been called magnetic percolation.

A characteristic feature of the reconnection scenario is that diffusion is not important everywhere but only at highly localized reconnection sites. But plasma transport can also occur in a broadly diffusive manner, as a result of mesoscale and microscale turbulence driven by instabilities that are either

local and microscopic in nature or that produce a cascade of energy to sufficiently small scales so that the frozen magnetic field condition can be broken.

A dilemma in magnetospheric physics is that no quantitative understanding has been reached concerning the relative importance of such diffusion and reconnection at the magnetopause. Calculations based on observed local mass flows in the LLBL and on its transverse scales have led to an estimated mass diffusion coefficient of the order of  $10^9 \text{ m}^2 \text{ s}^{-1}$  with an associated kinematic viscosity of the same order of magnitude. But assumptions concerning the magnitude of gradients and of the effective magnetopause entry area are built into such estimates, rendering them highly uncertain. Many theoretical predictions of the diffusion coefficient associated with specific unstable microscale and mesoscale wave modes also exist. They indicate difficulties in achieving values as high as  $10^9 \text{ m}^2 \text{ s}^{-1}$ .

Direct calculation of local mass diffusion from single-spacecraft observations is not practical because of the unknown irregular inward/outward motion of the magnetopause. In most cases, such motion completely dominates the sought-after diffusion velocity perpendicular to the magnetopause. It also prevents accurate determination of those gradients across the magnetopause and boundary layer that drive the transport. Estimates of the kinematic viscosity require determination of the correlation between normal and tangential velocity components at the magnetopause, (either from the distribution functions, in the case of microscopically based viscosity, or from macroscopic fluctuations), in the case of turbulent (eddy) viscosity. Such estimates are again compromised, or rendered invalid, by magnetopause motion. Another difficulty is that an extremely accurate vector,  $\mathbf{n}$ , defining the direction normal to the magnetopause is needed. The plasma velocity is mostly tangential to the layer so that even small errors in  $\mathbf{n}$  can significantly change the value of the diffusion velocity, i.e., the velocity component along  $\mathbf{n}$ , thereby seriously compromising the accuracy of transport coefficients derived from the data. Using a mission configuration (described in Section 2.3.1.2) with small spacecraft separation along  $\mathbf{n}$ , to obtain gradients and magnetopause motion, and larger separation in the magnetopause tangent plane, to obtain an accurate normal vector  $\mathbf{n}$ , including its temporal changes, the MMS mission will provide an excellent opportunity to obtain reliable mass diffusion and viscous diffusion coefficients applicable in the magnetopause regions.

### **2.3.4 Experimental Requirements for the MMS Turbulence Investigation**

Table 2.4 on the next page summarizes the measurement parameters and recommended interspacecraft distances for each of the three key science questions that constitute the MMS turbulence investigation. The orbital phases during which each questions will be addressed are also indicated.

<b>Question</b>	<i>What are the temporal and spatial properties of, and the physical processes responsible for, turbulence in the magnetosheath, magnetopause and plasma sheet?</i>	<i>What are the sources, propagation, and consequences of mesoscale boundary waves?</i>	<i>What is the role of turbulence in plasma entry through the magnetopause?</i>
<b>Orbit</b>	1.5 x 12 $R_E$ equatorial orbit with dayside apogee and transition to 1.5 x 30 $R_E$ nightside apogee (magnetosheath and magnetopause studies) 1.5 x 12 $R_E$ and 1.5 x 30 $R_E$ nightside apogee (plasma sheet study)	10 x 40 $R_E$ nightside apogee polar magnetopause skimming orbit	1.5 x 12 $R_E$ equatorial orbit with dayside apogee and 10 x 40 $R_E$ polar magnetopause skimming orbit with nightside apogee
<b>Spacecraft Separation Distances</b>	10 km to 1 $R_E$	10 km to 1 $R_E$	10 km to 1 $R_E$
<b>Measured Parameters</b>	<ul style="list-style-type: none"> <li>· High-frequency electric and magnetic fluctuations</li> <li>· Debye-scale plasma structures</li> <li>· Low-frequency electric and magnetic waves</li> <li>· High time-resolution electron and ion distribution functions</li> <li>· Ion composition</li> </ul>	<ul style="list-style-type: none"> <li>· Low-frequency electric and magnetic waves</li> <li>· High time-resolution electron and ion distribution functions</li> <li>· Ion composition</li> </ul>	<ul style="list-style-type: none"> <li>· High-frequency electric and magnetic fluctuations</li> <li>· Debye-scale plasma structures</li> <li>· Low-frequency electric and magnetic waves</li> <li>· High time-resolution electron and ion distribution functions</li> <li>· Ion composition</li> </ul>

**Table 2.4.** Measurement requirements for the MMS turbulence investigation.

### 3.0 The MMS Five-Spacecraft Cluster: the Need for Multipoint Measurements

The MMS mission requires at least four spacecraft in a tetrahedral formation in order to distinguish between spatial and temporal effects and to resolve the three-dimensional structure of the processes under study. However, the Science and Technology Definition Team recommends a baseline mission with five spacecraft, configured in either a hexahedral or “quad tetrahedra” formation (Figure 3.1). The addition of a fifth spacecraft will add relatively little to the cost and operational complexity of the mission but, as discussed in Section 3.2 below, will contribute significantly to the mission’s scientific yield. The separation between the spacecraft will vary from 10 km to tens of thousands of kilometers, allowing MMS to observe processes operating on the microscale and to relate these to larger-scale processes and structures.

#### 3.1 Separating Temporal and Spatial Effects Using MMS

Boundaries such as the magnetopause and the cross-tail current layer are in near-constant motion, with average speeds of  $\sim 10$ – $100 \text{ km s}^{-1}$ . As spacecraft usually have orbital speeds of  $1 \text{ km s}^{-1}$  or less at these altitudes, it is nearly always the in/out motion of the boundary or the propagation of a large-amplitude surface wave that causes the slowly moving spacecraft to rapidly cross these interfaces. Because of this boundary motion, it is impossible with a single spacecraft to obtain many of the key measurements necessary to understand magnetic reconnection, charged particle acceleration, and plasma turbulence. The rea-

son is that spatial gradients in the particles-and-fields environments of these interface regions appear in the instrument data as temporal variations when the boundaries move across the spacecraft. In such situations, the temporal variations that we need to measure and analyze are said to have been “aliased” by the presence of spatial gradients (or vice versa).

The aliasing problem is well-illustrated by the difficulties inherent in studying charged particle acceleration near the cross-tail current layer or the dayside magnetopause with single-point measurements. Populations of energetic charged particles from a variety of sources are always present near these boundaries. However, they are not always accelerated locally. As boundary motion carries the energetic particle layers over the spacecraft, variations in the particle fluxes are recorded by the instruments as a function of time. Thus, while an increase in particle flux measured as the spacecraft approaches the center of the boundary may imply that particles are being accelerated in the boundary (a temporal phenomenon), it may also simply indicate that their intensity is greatest near the center of the boundary (a spatial feature).

The solution to this spatial aliasing problem is to acquire data with multiple instruments distributed across a small network of spacecraft. From time delays in the appearance of variations in the particles-and-fields data, the direction and speed of the underlying boundary motion can be inferred and spatial gradients can be obtained directly. If the spacecraft are arrayed as a tetrahedron (the MMS hexahedron = two tetrahedra with a common base), these determinations can be made equally well for boundary motion in any direction (i.e., the “sensitivity” of

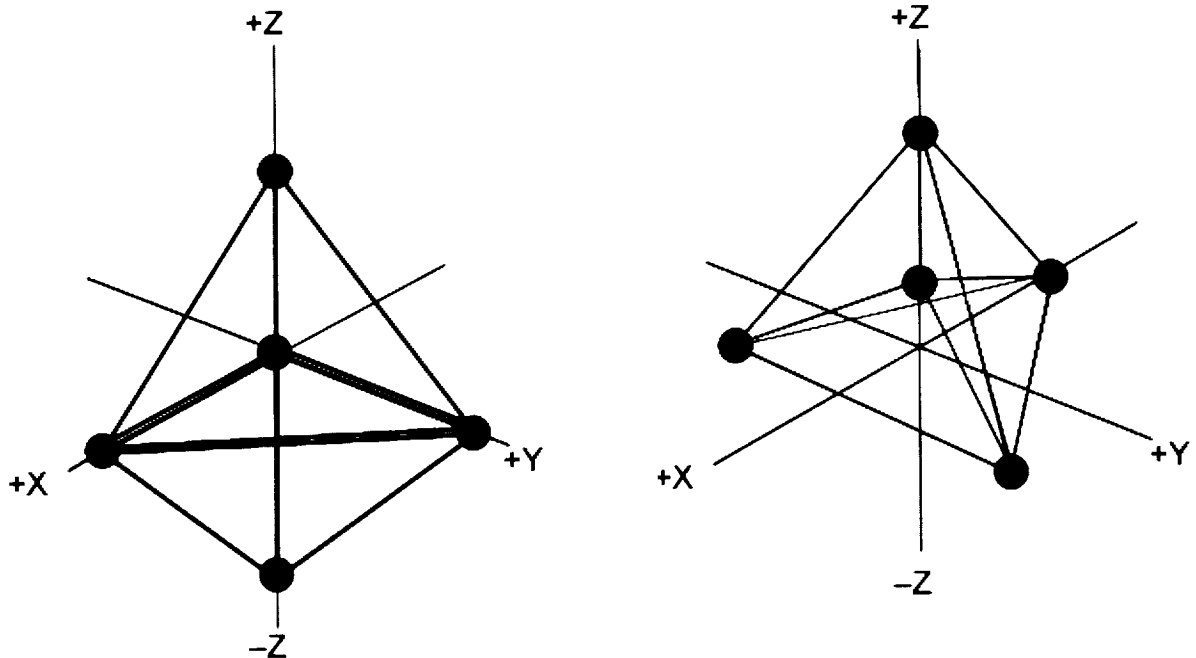


**Figure 3.1.** Two possible configurations for the five MMS spacecraft near apogee: a hexahedral configuration (left), comprising two tetrahedra, and a “quad tetrahedra” configuration (right). Within each of the tetrahedra, spatial gradients of the plasma and fields will be measured, from which  $\text{curl } \mathbf{B}$ ,  $\text{curl } \mathbf{v}$ , and  $\text{curl } \mathbf{E}$  can be derived. The five spacecraft will make it possible to determine the gradient of these derived quantities as well.

the technique is then not a function of the direction of boundary motion). This ability to obtain spatial gradients is essential to the MMS goal of understanding the fundamental physics of reconnection, particle acceleration, and turbulence. By measuring spatial gradients, for example, MMS will be able to determine the electric current density vector from the curl of the magnetic field across the multispacecraft tetrahedron. Knowledge of the current is essential for determining the local MHD stress balance within plasmas permeated by reconnected field lines, such as FTEs and plasmoids (see Section 2.1.4), and for establishing the local rate of energy generation or dissipation.

Conversely, identification of trends in the data caused by spatial effects will allow these effects to be corrected for and the true temporal variations in the charged particle and fields environments of the boundary regions to be determined. Important applications of these temporal variation measurements include (1) the observation of the onset of intense electric fields, fast plasma flows, and energetic particle acceleration, which signal the onset of reconnection, and (2) the cross-correlation of magnetic field temporal fluctuations from the arrayed spacecraft to create a “telescope” for observing low-frequency plasma waves and determining unambiguous propagation vectors and polarization.

### 3.2 Why a Five-Spacecraft Cluster?

Although the MMS mission could be flown with four spacecraft, the Science and Technology Definition Team has baselined a five-spacecraft mission rather than a four-spacecraft mission for three reasons.

First, a relatively closely spaced cluster of five spacecraft will enhance MMS’ ability to separate phenomena that vary in time from phenomena that are steady, but highly structured in space. As discussed in the preceding section, single spacecraft have no hope of distinguishing spatial from temporal effects. While even two spacecraft can separate space and time if they are not spaced too close to one another or too far apart relative to the spatial scale of the phenomena under study, variable separations and/or strings of spacecraft following the same track are needed to cover the different temporal regimes that are important for accomplishing the MMS science objectives. The ability to resolve spatial and temporal variability is improved as more spacecraft are added.

Secondly, five spacecraft in hexahedral formation will improve MMS’ ability to determine the structure and motion of plasma boundary layers and to identify the external conditions responsible for the boundary motion. In a three-dimensional system, such as the Earth’s magnetosphere, spatial structure can be determined by measuring plasma gradients along three orthogonal axes, X, Y, and Z. This measurement can be made with a set of four spacecraft, one of which is at the origin of a cartesian coordinate system with the other three along the X, Y, and Z axes, forming a tetrahedron. However, there is still a need to

know whether and how fast the boundary is moving and what the external conditions are that may be causing the boundary to move or change. The most common example of an external condition is the magnetosheath density and magnetic field vector just outside the magnetopause. Five spacecraft will therefore be required to determine spatial structure of a plasma boundary layer plus either the external conditions or the velocity of the boundary motion.

Finally, five spacecraft will create a “curlometer” that can measure the spatial gradients of plasmas and fields to derive important parameters such as currents (from  $\text{curl } \mathbf{B}$ ), plasma vorticities ( $\text{curl } \mathbf{v}$ ), and induced electric fields ( $\text{curl } \mathbf{E}$ ). The tetrahedral formation can make this measurement provided that the derived quantity (current, vorticity, etc.) is uniform in the space occupied by the cluster. In the nonuniform case, however, a fifth spacecraft is crucial because, by adding it outside the base of the tetrahedron, two back-to-back pyramids are formed (as a hexahedron) (cf. Figure 3.1) that can measure a spatial gradient of the derived quantities. As the hexahedron moves through space, temporal variations of the derived quantities can also be sensed. Alternatively, the fifth spacecraft could be placed inside the pyramid defined by the other four spacecraft, forming four tetrahedra internal to it. This “quad tetrahedra” configuration would then provide full vector gradients of the derived quantities over a small spatial scale.

## 4.0 Instrumentation

The five MMS spacecraft will be identically instrumented. Each will carry a payload consisting of two plasma instruments, an energetic particle detector, an electric field instrument, and a magnetometer. Achievement of the MMS science objectives requires that the instruments be capable of extremely high time resolution. This and other performance requirements are set forth for each type of instrument in the following paragraphs.

### 4.1 Plasma Instrumentation

The MMS plasma instrumentation should be capable of measuring three-dimensional composition-resolved distribution functions covering the energy/charge range from 1 eV to 40 keV with a time resolution of 0.75 second. The energy resolution ( $\Delta E/E$ ) should be approximately 20 percent, and the mass resolution ( $m/\Delta m$ ) should be at least 4. The geometric factors of the plasma instruments should be in the range of  $5 \times 10^{-4} \text{ cm}^2 \text{ sr}$  for electrons and  $1 \times 10^{-2} \text{ cm}^2 \text{ sr}$  for ions. The angular resolution of the data should be within  $10^\circ$  so that plasma flow velocities and field-aligned current densities can be determined. In order to achieve high time resolution for electron and ion distribution functions while at the same time obtaining good sensitivity for minor ions, a set of two plasma analyzers is suggested, with  $10^\circ \times 360^\circ$  fields of view oriented normal to the spin plane and separated by  $90^\circ$  around the spacecraft circumference so that complete three-dimensional distributions can be measured in one-fourth of a spin period.

## 4.2 Energetic Particle Detector

The energetic particle detectors carried by the MMS spacecraft should be capable of measuring 3D energetic ion distributions in the energy range of  $\sim 30$  keV to several MeV, and of determining major species (H, He, CNO group) ion composition. Electron distributions should be measured over the energy range of  $\sim 30$  keV to at least several hundred keV. The time resolution required is  $\sim 1.5$  seconds (one half of a spacecraft spin period). Good temporal, spatial, and spectral resolution are needed to characterize the structure and dynamics of magnetospheric boundary layers, and of the processes operating in particle acceleration regions. To provide the statistics for good temporal resolution in boundary layer studies, large geometry factors ( $\sim 0.1$  cm<sup>2</sup> sr) for each instrument look direction are highly desirable. An example candidate instrument would be a new generation compact TOF  $\times$  E spectrometer. These have a fan-shaped field of view of  $\sim 10^\circ \times 160^\circ$ , and very good geometry factors. Two such heads could provide full 3D coverage twice per spin, with low mass, power, and volume requirements. This measurement technique has much recent flight experience (AMPTE, Galileo, ISTP, etc.). A dedicated electron head using imaging, multistrip sensor technologies (as on POLAR, CLUSTER, etc.) would also be possible and desirable. Data would be binned and compressed in the instrument DPU to provide the temporal resolution appropriate to the science requirements in each spacecraft data mode. Pre-launch calibration would be maintained by in-flight calibration sequences and by interspacecraft comparisons in regions of uniform flux.

## 4.3 Electric Field Instrument

Each MMS spacecraft should carry a three-axis DC electric field instrument and plasma wave receiver. The role of the electric field and wave instrument is (1) to determine changes in the perpendicular (e.g., fast flows) and parallel electric (e.g.,  $\Delta E_{\parallel}$ ) field signatures as evidence of the reconnection diffusion region, (2) to detect and characterize both quasi-static and transient spatial structures of multiple scale sizes from the Debye length to  $\sim R_E$  and to characterize plasma waves from Alfvén frequencies to the local plasma frequency in the outer magnetosphere to investigate turbulence, and (3) to determine the potential of large scale structures to investigate particle acceleration. The electric field measurements will also be used to measure plasma drift velocities, local plasma density, and spacecraft potential. The capabilities of the electric field instrument should be similar to (or better than) those of the Polar

instrument, with the goal to obtain  $\sim 1$  mV/m on spin-averaged, perpendicular electric fields,  $\sim 3$  mV/m on  $\Delta E_{\parallel}$ , and  $\sim 1 \times 10^{-14}$  (V/m)<sup>2</sup>/Hz at 100 kHz spectral power density. One approach is to use 80-meter tip-to-tip double probes in the spin plane, and  $>10$ -meter tip-to-tip axial masts. It is recognized that the accuracy of the measurement (depending upon magnetic orientation) depends upon the length of axial masts. If sufficient mass and stability margins are available, 20-meter tip-to-tip axial masts are desirable. In addition, to determine the magnetic component of plasma waves with frequencies ranging from 25 Hz to several hundred kHz, a search coil antenna system could be deployed on a boom positioned to offset the magnetometer boom. The search coil would share electronics with the E-field instrument. (This option is included in the spacecraft design presented in Section 8.1 and in the spacecraft mass estimate given in Table 8.1.)

## 4.4 Magnetometer

A candidate magnetometer for Multiscale Mission is a dual triaxial magnetometer using ring core fluxgate magnetic sensors. These low-noise sensors are derived from the same technology used on the ISEE, Pioneer Venus, Voyager, Galileo, GGS, and Cassini missions. A dynamic range of 60,000 nT with a digitization of  $\sim 1$  nT on one of these two triaxial sensors and a  $\sim 600$  nT with a resolution of  $\sim 10$  pT on the other triaxial sensor would cover the full range of field strengths with the resolution required. The vector magnetic field should be sampled at a rate of at least 100 vectors per second. These data can be averaged to lower rates over much of the trajectory but are needed for periods of burst mode collection. The sensors should be mounted on a stable boom so that any time varying spacecraft fields are less than 0.1 nT. The relative timing of samples should be known on the multiple spacecraft to better than 1 ms if the spin period is 4 seconds and proportionately better for shorter periods. The orientation of the spin axes of the spacecraft and their spin phase should be known to within  $0.1^\circ$ . A magnetic cleanliness program during the design, fabrication, integration and test phase is an essential adjunct to the magnetometer investigation. If these requirements are met, intercalibration techniques using quiet field regions of the magnetosphere can provide extremely accurate intercalibration of the multiple magnetometers. The ability to tilt the spin axes of one or more of the spacecraft to check the zero levels of the other sensors is a useful feature. Continuous operation of the spacecraft with spin axes at significant ( $>45^\circ$ ) angles offers many advantages to both the fields and plasma investigations.

## 5.0 Phases of the MMS Mission

The nominal MMS mission has an operational duration of two years. It will be conducted in four phases, which are defined by changes in the orbital parameters. In each phase, the three fundamental processes—reconnection, particle acceleration, and turbulence—will be studied in different magnetospheric settings. In Phases 1 and 2, the spacecraft cluster will be in a  $10^\circ$ -inclination orbit. During Phase 1, the scientific emphasis will be on processes occurring at the low-latitude dayside magnetopause and on substorm-related processes in the near-Earth magnetotail. Phase 2 will focus on the investigation of the dawnside flank of the equatorial magnetopause and the magnetotail at distances up to  $30 R_E$ , with special interest in substorm onset and evolution. Phase 3 will use lunar swing-bys to take the spacecraft out to  $120 R_E$  in the deep tail and then to rotate the plane of the orbit to become perpendicular to the plane of the ecliptic. During this phase MMS will investigate plasmoid evolution and the nature of merging at the distant neutral line. Phase 4 will be conducted from the  $90^\circ$ -inclination orbit achieved through the rotation of the orbital plane during Phase 3 and will focus on the investigation of the entire dayside magnetopause, which it will skim from north to south, with additional interest in studies of the mid-tail. Specific details of each mission phase are given in the paragraphs that follow.

### 5.1 Phase 1: Dayside Magnetopause/Near-Earth Magnetotail Investigation

The nominal subsolar distances to the bow shock and magnetopause are  $15 R_E$  and  $10 R_E$ , respectively. With an apogee of  $12 R_E$  during Phase 1, the MMS spacecraft will sample the low-latitude magnetopause over a range of local times around noon with excursions into the magnetosheath. As upstream conditions vary, multiple magnetopause crossings will occur. When apogee is on the night side, the focus of the investigation will be on substorm-related phenomena, such as the evolution of the current sheet and earthward plasma flows in the near-Earth tail. As illustrated in the diagram in **Figure 5.1**, Phase 1 will last nine months, with the evolution of the orbit taking the spacecraft cluster from an initial apogee at 0340 local time, across the magnetotail, and around to the dayside magnetopause.

Since the Earth's magnetic field dominates at close distances, the Phase 1 orbit has been designed so that its line of apsides lies close to the magnetic equator. The orbital period will be adjusted to be exactly synchronous. The argument of perigee for Phase 1 is  $0^\circ$ . As a result, apogee and perigee will occur over the intersection of the geomagnetic and geographic equators (i.e., at  $\sim 15^\circ$  E or  $156^\circ$  W).

### 5.2 Phase 2: Near-Earth Neutral Line/Magnetopause Flanks Investigation

Primary emphasis during Phase 2 of the mission will be on processes occurring in the region of the near-Earth neutral line, i.e., between  $20$  and  $30 R_E$ . In order to explore this region in the magnetotail, orbit apogee will need to rise, as illustrated in **Figure 5.2**. As apogee is raised, MMS will be able to explore the dawn flank of the magnetosphere, with excursions through the low-latitude boundary layer (LLBL) back and forth across the magnetopause. As the orbit traverses the magnetotail, the MMS cluster must

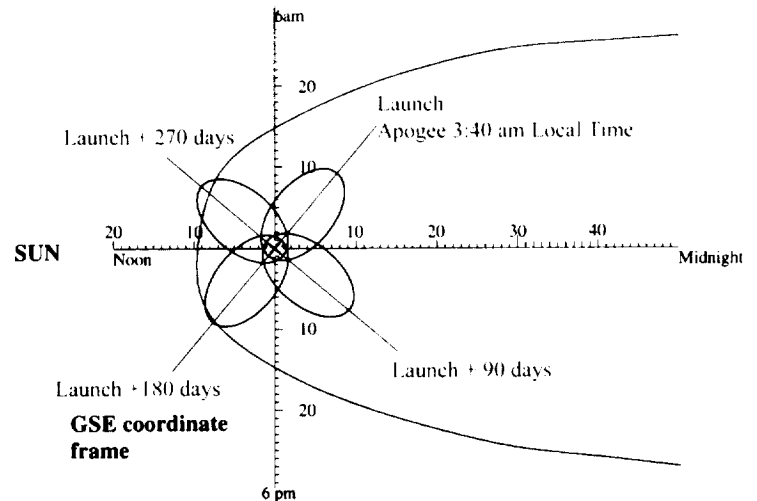


**Figure 5.1.** During Phase 1, MMS orbit apogee will occur at a radial distance of  $12 R_E$  and will precess over a nine-month period from 0340 local time, through the midnight meridian, around to the dayside magnetopause. Orbit inclination during this phase is  $10^\circ$ . The focus of the science investigation during Phase 1 will be on the evolution of the current sheet in the near-Earth tail during substorms and on magnetic merging at the subsolar magnetopause.

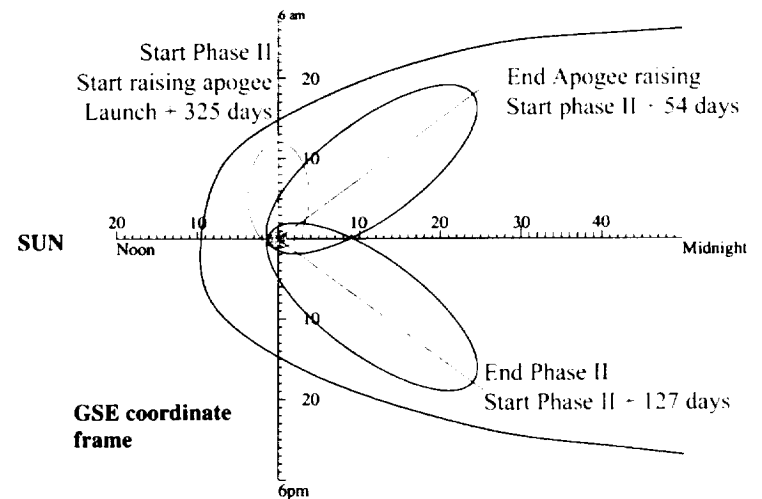


**Figure 5.2.** During Phase 2, the MMS orbit apogee will be gradually lengthened, from  $12$  to  $30 R_E$ , and will continue to precess in local time. The focus of the investigation will shift during this phase to processes occurring at the magnetopause flanks and in the LLBL and to reconnection at the near-Earth neutral line, which is located in the tail between  $20$  and  $30 R_E$ .

remain close to the plasma sheet for as long as possible in order to achieve the maximum scientific yield. Balancing the requirement to be close to the plasma sheet with the engineering requirement to avoid long eclipses places a seasonal time constraint on the optimal orbit. To avoid long shadows, and to maximize the amount of time that the spacecraft spend in the plasma sheet, it is best to cross the midnight meridian at a time when the plasma sheet is displaced from the GSM equatorial plane (i.e., around the June or December solstice) when the tilt angle is largest in magnitude. If the mission orbits are designed such that either June or December corresponds to the midnight position as shown in **Figure 5.2**, then the launch windows can be determined by stepping backwards in time from either of those dates.

### 5.3 Phase 3: Distant Magnetotail Studies

Phase 3 is primarily an orbit transition phase in which the gravitational pull of the Moon will be used to increase the perigee and apogee distances and then to induce a  $\sim 90^\circ$  orbit plane change. These maneuvers will be accomplished on the night side of the orbit so that the spacecraft will make deep passes into the distant tail ( $\sim 100$ - $120 R_E$ ) to conduct science investigations of that region. Two sets of double-lunar-swing-by (DLS) maneuvers will be performed to effect the change from low- to high-inclination orbit. In order to complete all phases within the planned mission lifetime, the duration of the DLS will be no longer than one month.

### 5.4 Phase 4: Magnetopause Skimming/Mid-Tail Investigation Phase

By the end of Phase 3, the inclination of the MMS orbit will have increased to  $90^\circ$  and the perigee and apogee will have been raised to  $10 R_E$  and  $40 R_E$ , respectively. Apogee will be on the night side. This orbit will allow MMS to skim the magnetopause from pole to pole during Phase 4 and to make observations in the previously underexplored high-latitude magnetopause environment. On the dayside, MMS will sample the cusp/cleft regions as well as subsolar and high-latitude reconnection sites under changing IMF orientations. On the night side, north-south cuts of the plasma sheet in the mid-tail will provide information on the dynamics of the plasma sheet. Finally, traversals of the high-latitude boundary layer will allow MMS to investigate the transport of solar wind plasma across the magnetopause.

## 6.0 MMS Spacecraft Separation Strategies

As described below, the distances separating the five MMS spacecraft will vary from 10 kilometers to a few thousand kilometers to a few  $R_E$  throughout the mission, with the separations sometimes decreasing and sometimes increasing as a particular orbital phase evolves. It is this feature that gives MMS its "multiscale" character and that will make it possible to relate the plasma micro-processes that are the focus of the MMS investigation to meso- and macroscale phenomena.

Phase 1 ( $12 R_E$  apogee,  $10^\circ$  inclination): apogee starts at about 03 MLT and swings through midnight and then to noon. The hexahedron/quad tetrahedron forms at apogee. Separation starts at 1000 to 2000 km and are reduced to 10 km for a few weeks when

apogee is near midnight. The separation is then increased again to 1000-2000 km. After apogee crosses the dusk meridian, the separation is reduced, becoming 10 km at noon.

Phase 2 (Near-Earth Neutral Line/Magnetopause Flank Study): the separation is increased as apogee moves through the morning hours, becoming a few thousand kilometers at 03 MLT. It is then reduced to 1000 km around midnight ( $30 R_E$  apogee) before being increased again to a few thousand kilometers at 21 MLT.

Phase 3 (Deep Tail Study): Separation will increase to a few  $R_E$  with some orbits in a string of pearls configuration.

Phase 4: ( $10 \times 40 R_E$ , polar orbit). A hexadron/quad-tetrahedron with separations of a few thousand kilometers would be formed at apogee, with a string of pearls evolving as the dayside perigee is approached.

## 7.0 Orbit Insertion and Formation Flying

The five MMS spacecraft are to be launched from a single vehicle. Because of the high altitude of the MMS orbit and the limited mission budget, launch vehicle options are constrained to Delta II class vehicles. For the preliminary study presented in this report, launch on a Delta II 7925H with 10' fairing has been assumed (**Figure 7.1**). (There are more capable foreign carriers that are within the MMS budget requirements. The viability of such options will be assessed in the coming months.)

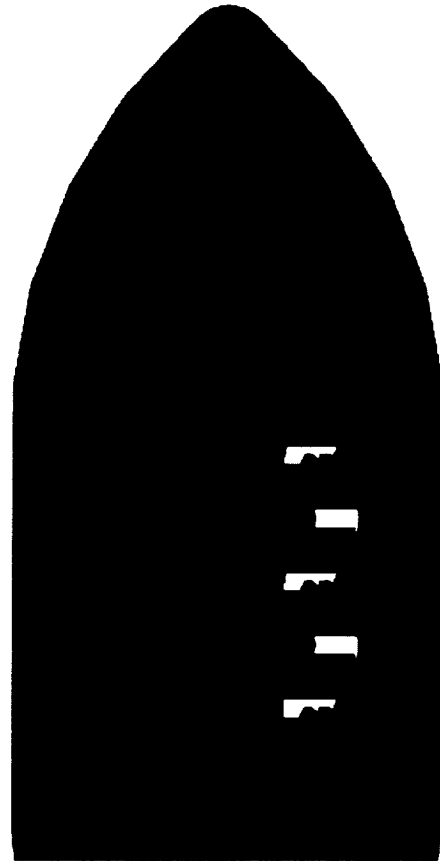


**Figure 7.1.** The five MMS spacecraft are shown here in stacked configuration, mounted inside the 10' fairing of a Delta II 7925H launch vehicle.

Two orbit insertion scenarios were evaluated to determine which would deliver the most mass to the Phase 1 orbit. In the first scenario, the launch vehicle deposits the five MMS spacecraft directly into the  $1.2 R_E \times 12 R_E$   $10^\circ$ -inclination Phase 1 orbit; in the second scenario, the five spacecraft are put first into a  $28^\circ$ -inclination parking orbit from which they then use on-board propulsion to perform the final maneuver into the Phase 1 orbit. Scenario 1 requires that the launch vehicle carry a fourth-stage kick motor to achieve the final inclination, resulting in a loss in efficiency. Scenario 2 is therefore preferable. Each spacecraft needs to provide  $\sim 330 \text{ m s}^{-1} \Delta V$  to perform the inclination change. The total mass delivered to the parking orbit is estimated to be  $\sim 1540 \text{ kg}$  or roughly  $308 \text{ kg}$  per spacecraft. (These values are based on the current best estimate of spacecraft mass, as given in **Table 8.1**, plus a 20% margin.) The  $1540 \text{ kg}$  total mass value does not include the mass of the Payload Attach Fitting (PAF), as noted in **Table 8.2**. With the expenditure of fuel needed to perform the inclination-change maneuver (hydrazine propellant is assumed), the total mass of the cluster upon arrival in the Phase 1 orbit will be  $\sim 1305 \text{ kg}$  ( $\sim 261 \text{ kg}$  per spacecraft).

Once the MMS spacecraft have been placed into orbit, the parameters of the individual spacecraft orbits have been designed so that the configuration of the five-spacecraft formation will evolve during the orbit to form a specified hexahedron/quad tetrahedron near apogee. The flight formation results from the initial conditions of the orbit and does not require any action by the spacecraft. The hexahedron/quad-tetrahedron will evolve in a deterministic manner throughout the orbit, becoming fairly elongated along the orbit at lower altitudes.

## 8.0 The MMS Spacecraft

The MMS mission design calls for five identical spacecraft with identical science payloads. The baseline science instrumentation (see Section 4.0) utilizes proven, relatively straightforward designs employing currently available technology. As far as spacecraft technology is concerned, no new mission-enabling technologies are required: the MMS mission could be conducted with technologies in existence today and meet the baseline science requirements. However, certain mission-enhancing technologies currently under development—such as an interspacecraft ranging and alarm system (IRAS), phased-array antennas, and advanced conductive solar arrays—would improve performance and reduce costs and/or complexity.

The following sections describe a strawman spacecraft design. This design meets both the scientific and the engineering requirements of the MMS mission.

### 8.1 Spacecraft Configuration

The strawman MMS spacecraft has been configured for maximum simplicity and ease of packaging. Each spacecraft is a spin-stabilized flat structure with the form of a regular octagon when viewed from either end and with a very stable height-to-diameter ratio (**Figure 8.1**). Because the upper stage of the launch vehicle will be spin-stabilized, the five spacecraft must be balanced in their launch configuration (cf. **Figure 7.1**), and the center of gravity of the spacecraft stack must meet the requirement specified in the launch vehicle user's guide. This stacking and balancing requirement has led to the proposed flat design for the spacecraft bus. This design, in turn, necessitates

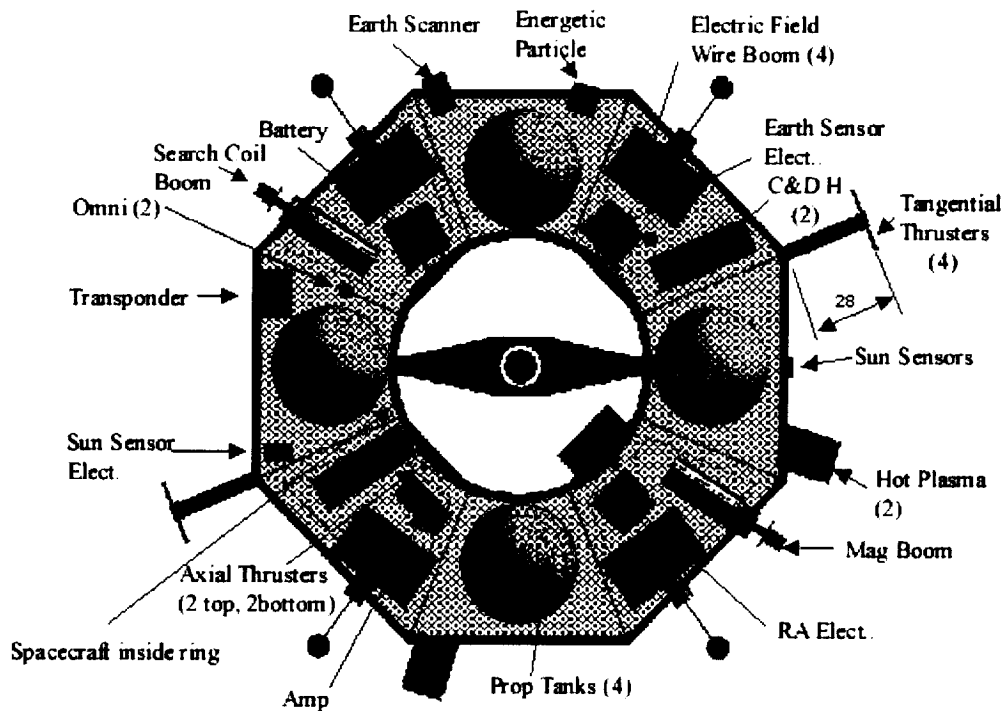


**Figure 8.1.** View of the MMS payload deck, showing the location of the various instruments and spacecraft subsystems. The MMS design uses an open architecture to facilitate instrument and subsystem integration and to provide ease of access, even when the five spacecraft are in stacked launch configuration. The spacecraft octagon measures  $109''$  from apex to apex and  $19''$  in height (not including deployed solar array petals).

<u>Quantity</u>	<u>Component</u>	<u>(kg)</u>	<u>Mass (kg)</u>	<u>Dimensions (in)</u>	<u>Comments</u>
4	E-Field -Radial	2	8	8 x 5 x 13	4" Protrusion o/s s/c
2	E-Field -Axial	2.5	5	4.5 diam x 11.5	Top & Bottom Decks
1	E-Field -Electronics	2	2		Inside s/c
2	Hot Plasma	8	16	6.0 dia x 4.0	Faces O/S 90 degrees
1	Mag + Boom	2.5	2.5	7 x 4 x 3	Faces O/S
1	S-Coil Mag + Boom	2.5	2.5	7 x 4 x 3	Faces O/S
1	Energetic Particle	2	2	4 dia x 4	cyl. side faces O/S
8	Ranging Antennas	0.1	0.8		6 trans, 2 receive
1	R. A. Electronics	1.5	1.5	4 x 8 x 6	Inside s/c
2	Omni Antenna	0.5	1	4 x 2 dia.	top and bottom
1	Xpondr X-band	3.1	3.1	6.8 x 5.3 x 4.5	Inside s/c
1	Comm Amplif	2.17	2.17	6.5 x 6.5 x 6.5	Inside s/c
1	Other Comm Stuff	3.37	3.37		Inside s/c
1	Earth Sensor	0.77	0.77	5.25 x 3.6 OD	Faces O/S
1	Earth Sensor Elec.	1.77	1.77	6 x 7 x 3.25	Inside s/c
2	Sun Sensor	0.109	0.218	2.6 x 1.3 x 1	Faces O/S
1	Sun Sensor elec.	0.726	0.726	4 x 2.3 x 3.7	Inside s/c
1	Prop Tanks/Plumb.	19.86	19.86	16.5 dia, 1840 in <sup>3</sup>	4 tanks+ 15% plumbing
8	1# thruster+valve	0.34	2.72		
1	Thermal	3.5	3.5	N/A	Blankets & T'stats
1	C&DH box	11.5	11.5	1 0x 14.63x 11.13	+pyro, EVD cards
1	S/C Harness	6	6		mostly on lower deck
1	Battery	7.7	7.7	7.2 x 7.2 x 7.2	Inside s/c
1	Power System Elec	5.4	5.4	12 x 12 x 4	Inside s/c
1	Solar Array	4.2	4.2	2.32 m <sup>2</sup>	cells only, 1.8 kg/ m <sup>2</sup>
1	Separation Device	5.9	5.9	37" v-band	at upper ring I/F
1	Structure	42	42		composite + cell substrate
1	Fuel	95.72	95.72		1000 dv
	Probe S/C		257.93		
	Total				

**Table 8.1.** As shown in this table, the best estimate for the MMS spacecraft mass budget (without the 20% margin) is 257.93 kg.

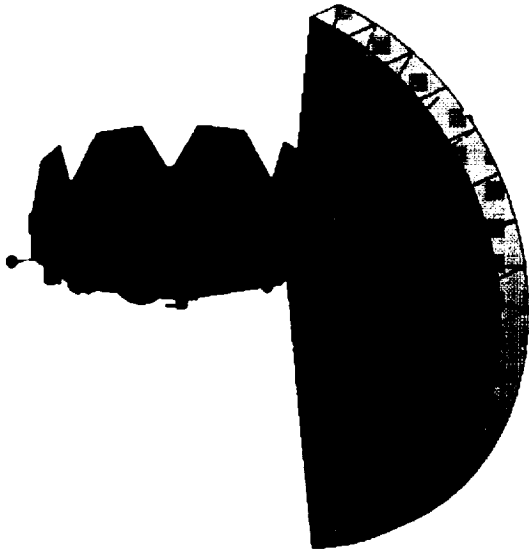


**Figure 8.2.** This 3-D view of the MMS spacecraft shows the eight solar array petals in deployed position and the fan-shaped field of view of the energetic particle detector.

the addition of a mechanism to deploy eight petal-shaped solar array panels (**Figure 8.2**) to increase the on-orbit solar array area to meet the power needs of the spacecraft and the instruments. As illustrated in **Figures 8.2** and **8.3**, the instruments are positioned on the payload deck such that the fields of view for all instruments are clear and the boom deployments are unimpeded.

In the strawman design, the load-bearing element of the spacecraft is a central interior tube or ring around which the instruments and spacecraft subsystems are positioned on the payload deck. When the spacecraft are stacked one on top of the other in launch configuration, these rings will form a very strong cylindrical structure well capable of carrying the vehicle launch loads. The diameter of the inside ring is designed to match the diameter of the payload attach fitting of the launch vehicle, resulting in a simple, straightforward load path.

The baseline MMS spacecraft has been configured as an open structure to facilitate integration of the instruments onto the spacecraft and to provide access to the instruments after integration without disassembly of the spacecraft. This open architecture is particularly advantageous because it will allow access to at least some components when the five spacecraft are integrated together in stacked configuration for part of the mission-level integration and test activity.

**Table 8.1** provides a detailed mass breakdown for the baseline MMS spacecraft, while **Table 8.2** indicates the mass margin against the launch vehicle capability. The functional block diagram in **Figure 8.4** illustrates the strawman mission system architecture.

## 8.2 Attitude Control System (ACS)

The MMS spacecraft must be spin-stabilized, with a nominal spin rate of  $20 \pm 0.2$  rpm and a spin axis knowledge of better

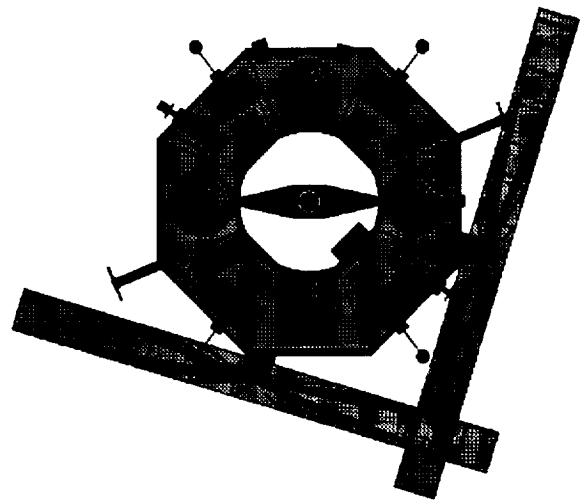


**Figure 8.3.** Top view of the spacecraft, showing the fields of view of the two (non-scanning) plasma instruments.

than  $0.1^\circ$ . Only “loose” control of the spin axis normal to the ecliptic plane ( $\pm 5^\circ$ ) will be required for the science observations. The spacecraft spin axis will be canted  $\sim 2^\circ$ - $5^\circ$  from ecliptic normal to prevent shadowing of the electric field boom sensors. In addition to basic orbit maintenance maneuvers, numerous in-plane and out-of-plane orbit maneuvers will be required during the mission. The first—and most significant from the standpoint of the  $\Delta V$  required—is the out-of-plane maneuver to change the inclination of the orbit from the  $28^\circ$ -inclination parking orbit to the  $10^\circ$ -inclination Phase 1 orbit (see Section 6.0). The instruments will be unpowered (except for heaters) during this initial plane change maneuver. At the end of Phase 1, in-plane apogee raising maneuvers will be performed to bring the MMS cluster into the Phase 2 orbit. As discussed in Section 5.1.3, two complicated double-lunar-swing-by maneuvers will be performed in Phase 3 to achieve the  $90^\circ$ -inclination Phase 4 orbit. The ACS will maintain the proper attitude of the spacecraft to allow data taking throughout all the maneuvers except the initial plane change.

5 Probe S/C	1289.65
3712 PAF	0
<b>MMS Mission Total</b>	<b>1289.65</b>
7925H-10 Vehicle capability	1540
Margin (kg)	250.35
Percent Margin	19.4%

**Table 8.2.** Mass margin relative to the capacity of the Delta II 7925H Payload Attach Faring (PAF) mass not included).

# Mag-Multiscale Architectural Diagram C&DH

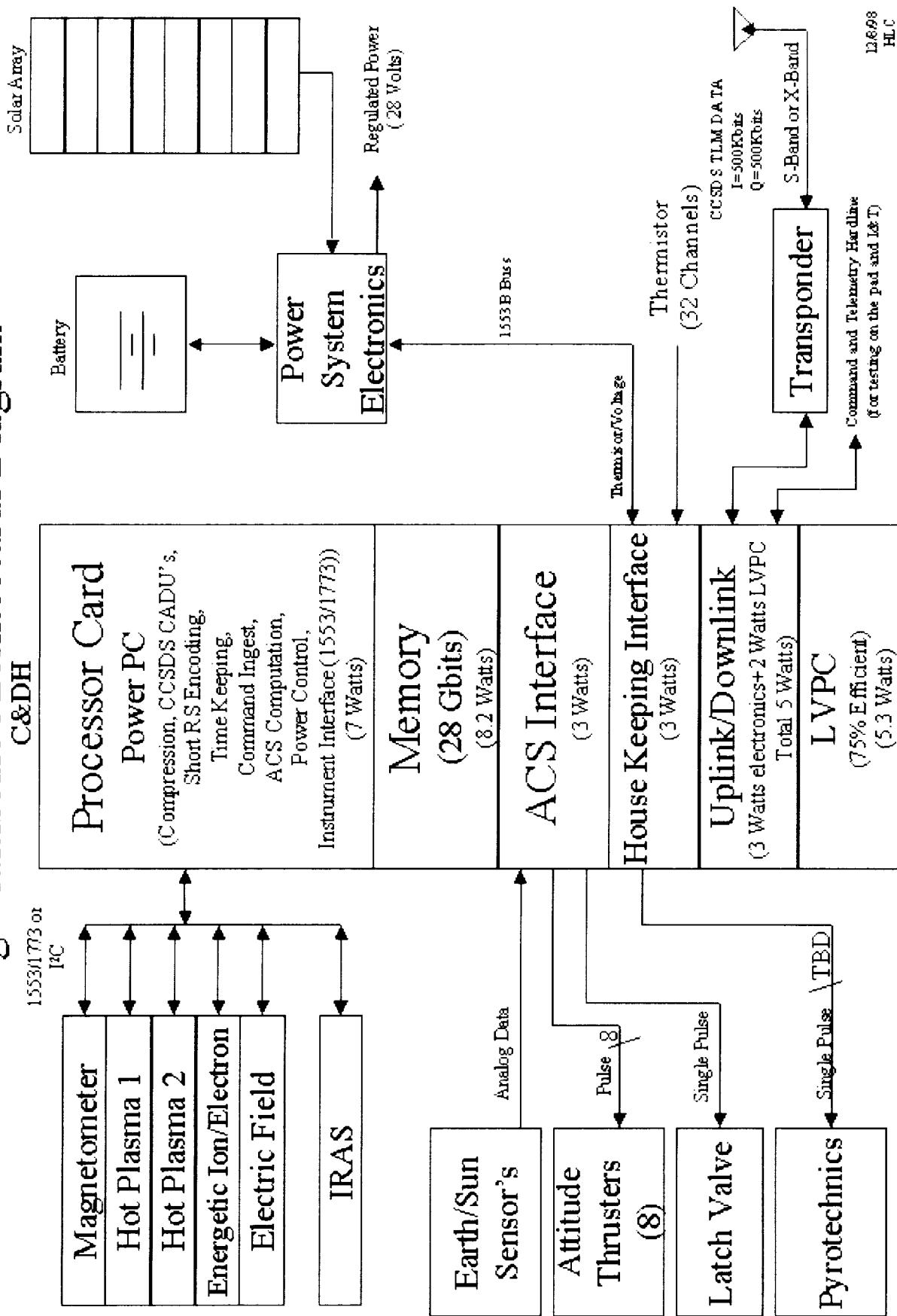


Figure 8.4. Block diagram illustrating the system architecture for the MMS spacecraft.

Parameter	Value	Remarks
Spacecraft EIRP	14.0dBW	
Polarization loss	-0.3dB	
Free space loss	-205dB	50000 km at 8.450GHz
Atmosphere + rain loss	-4.7dB	99.9% coverage at 5° el
Groundstation G/T	33dB/°K	11m 55% efficient
Data rate	60dB-bps	1Mbps
Received Eb/N0	5.69dB	
Implementation loss	1.0dB	
Required Eb/N0	2.6dB	R-S + rate ½ BPSK BER=10-5
Margin	2.0 dB	

**Table 8.3.** Commercial 11-meter dishes will be used for communications with MMS during Phases 1 and 2. 11-meter dish can communicate to 50000 km at 1 Mbps. Value given in table represent worst case assumptions.

Parameter	Value	Remarks
Spacecraft EIRP	14.0dBW	
Polarization loss	-0.3dB	
Free space loss	-227dB	100 R <sub>E</sub> at 8.450GHz
Atmosphere + rain loss	-0.08dB	30° el
Groundstation G/T	52.2dB/°K	34m 55% efficient
Data rate	61.76dB-bps	1.5Mbps
Received Eb/N0	5.61dB	R-S + rate ½ BPSK BER=10-5
Implementation loss	1.0dB	
Required Eb/N0	2.42dB	
Margin	2.2 dB	

**Table 8.4.** DSN 34-meter dishes will be used for communication with MMS during Phases 3 and 4. 34-meter dish can communicate to 100 R<sub>E</sub> at 1 Mbps. (Values shown represent nominal case assumptions.)

There is a complex interrelationship among the spacecraft spin rate, the ability of the ACS to achieve the 0.1° pointing knowledge, and the ability of the hot plasma instrument to provide the required 0.75-s time resolution. This interrelationship has implications for the design of both the ACS and the hot plasma detector. At the nominal spin rate of 20 rpm, the hot plasma analyzer can achieve the required time resolution with a fixed field of view—that is, without scanning. Use of a fixed field of view greatly simplifies the design of the instrument. However, at that high rate of spin, traditional star trackers appear not to be able to perform well enough to meet the knowledge requirement of 0.1° about the spin axis. On the other hand, if the spin rate is lowered to a rate at which a star tracker will perform as required (i.e., <6 rpm), then the hot plasma detector must employ electronic scanning in order to achieve the need time resolution. A study is therefore currently under way to assess star tracker performance and to identify alternatives to star trackers, such as steerable horizon-crossing sensors and star scanners.

### 8.3 Data and Communication System

The MMS spacecraft will use an X-band frequency for uplink and downlink. The uplink and downlink telemetry will be in the Consultative Committee for Space Data Systems (CCSDS) Advanced Orbiting Systems (AOS) format. Commanding for the instruments is estimated to be 100 bytes per instrument per day for each spacecraft.

The instrument complement will generate ~2 Gbits per day per spacecraft. Because the range to the ground stations will be relatively close during Phases 1 and 2, commercial stations with 11-meter dishes (**Table 8.3**) will be used for spacecraft-to-ground communications during these two phases. However, for communication during Phases 3 and 4, the DSN 34-meter dish will be needed (**Table 8.4**). In order to minimize ground station cost, the spacecraft must be able to store up to two weeks' worth of science data without loss until the range to the ground station is short enough to allow the data to be transmitted at a high rate (at least 1 Mbps but less than 2.2 Mbps).

In order to minimize system costs, the spacecraft must be capable of transmitting an EIRP of at least 14dBW in the direction of the Earth. It is assumed that the transmitter will be capable of transmitting continuously for at least four hours.

In order to analyze and interpret the MMS science data it is vital that the shape and orientation of the five-spacecraft formation at the time of data acquisition be known. This knowledge will be obtained by tracking the spacecraft as they progress through their orbits and then reconstructing the configuration of their formation on the ground. Methods for tracking the spacecraft and determining their orientation are currently under study. Two options are being considered: two-way Doppler ranging and one-way Doppler ranging using the signal from high-stability oscillators on board each spacecraft. Two-way (coherent) Doppler is the current baseline, with a requirement of 100-km spatial resolution of the cluster position for normal operations.

### 8.4 Power System

The MMS instrument complement requires ~39 W of power at 28 V. The spacecraft requires an average power of ~94 W on the day side and ~103 W on the night side. Thus the total power requirement is ~133 W during the daylight portion of the orbit and ~142 W during eclipse (see **Table 8.5** for the detailed power budget breakdown). To meet these power requirements, dual-junction GaAs cells with an assumed efficiency of 21percent will be used, covering a total area of the spacecraft of 2.32 m<sup>2</sup> (0.29 m<sup>2</sup> per facet x 8 facets). This design yields adequate margin for all power load cases. For the strawman spacecraft design presented here, it is assumed that the maximum eclipse duration would be 2 hours. Under this assumption, a 26-Ah battery will be sufficient to satisfy spacecraft power needs during eclipse, if the depth of discharge is limited to 40%. A lithium ion battery has been baselined to minimize the weight and volume impact (7.3 kg, ~7 in<sup>3</sup>). Although lithium ion batteries of this size are not currently available, it is anticipated that they will be readily available in time for MMS spacecraft development. If not, a NiH2 battery would suffice.

### 8.5 Interspacecraft Ranging and Alarm System (IRAS)

A unique feature of the MMS mission is that the five spacecraft together form a single sensor that can measure the **div**, **grad**, and **curl** of the electric and magnetic fields directly. In order to calculate these vector quantities, the distances between the spacecraft must be known to better than 1% of the separation between the spacecraft. The interspacecraft distances will be changed throughout the mission to match the scale size of the phenomena being investigated and will vary from 10 km to several tens of thousands of kilometers (see Section 6.0 above). To determine interspacecraft distances less than 100 km, the strawman design calls for an Interspacecraft Ranging and Alarm System (IRAS) on each spacecraft that will continuously monitor the distance among the spacecraft and record that distance during science operations or when an alarm flag is set. The IRAS will employ an RF antenna on each spacecraft and will send a low-speed serial message to the C&DH system. This message will contain the following information: distance to the other spacecraft in the formation, alarm status of each spacecraft, thruster firing status of each spacecraft, and internal IRAS health and safety. The IRAS will also provide timing information to within 50 ms, allowing for

highly accurate correlation and intercomparison of the data acquired by the five individual spacecraft. A technology program to develop the proof-of-concept hardware for the IRAS is currently under way. However, in view of the possibility of an accelerated development and launch schedule for MMS (see Section 10) and given the innovative and unproven nature of the IRAS, an alternative back-up concept to provide the ranging data is also being developed. The proposed back-up system will employ several ground stations for improved tracking data and post-processing activities to remove correlated error terms. Further analysis of the proposed back-up system is needed in the coming year; however, preliminary evaluation of this option indicates that it represents a viable alternative to the IRAS, though it complicates mission operations somewhat by reducing spacecraft autonomy.

### 9.0 Mission Lifetime and Reliability

The MMS mission concept has been optimized so that required measurements can be taken at the necessary locations within the magnetosphere within the specified two-year mission lifetime. The mission design calls for the deployment of a “virtual sensor” consisting of five spacecraft. This concept allows for implementation of an aggressive spacecraft design philosophy to maximize design simplicity and minimize redundancy and still ensure that the science goals will be met. The overarching reliability goal is to have at least four spacecraft still operating at the end of the two-year mission lifetime. If there is fuel remaining after the nominal end of mission, then measurements can continue in an extended mission with the spacecraft cluster in the Phase 4 orbit until the fuel has been completely consumed. Expendables will be sized to support 1,100 m s<sup>-1</sup>.

### 10.0 Mission Schedule

The MMS launch is currently scheduled for June of 2006 (see figure 10.1). NASA is working on a new initiative: Living with a Star. Part of that initiative includes accelerating the launch dates of the STP mission. The impact to MMS could be a move up of the launch date by 6 months. A decision on that should come in the summer of 2000. The impact on the MMS schedule would be a shortening of the formulation phase by 6 months. The baseline schedule, as depicted in figure 10.1, shall be used for planning and costing purposes until other direction is given.

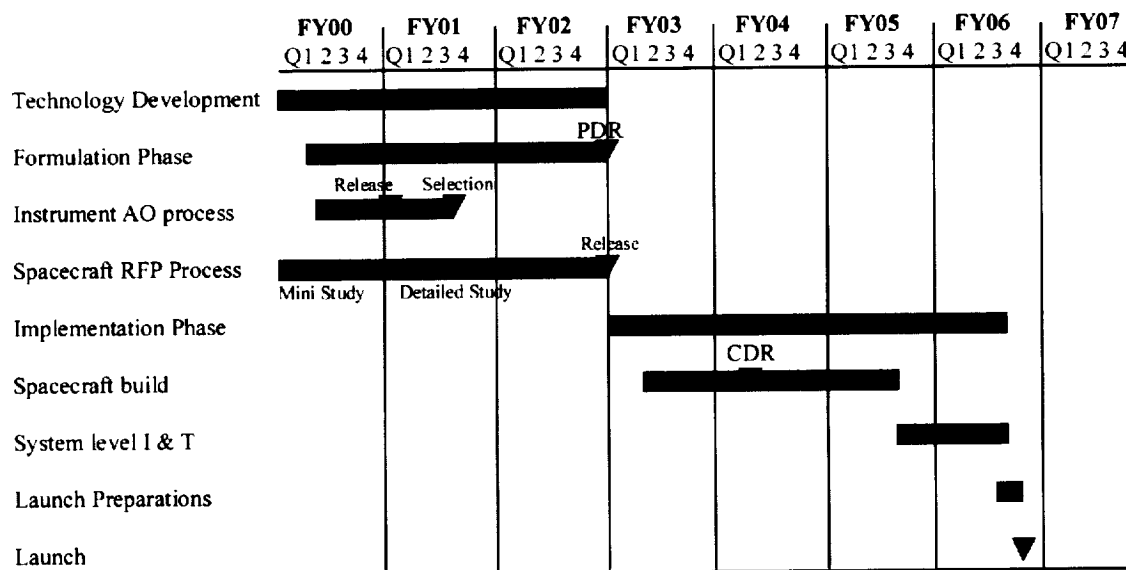


**Figure 10.1.** MMS launch is currently scheduled for September 2006. However, because no new mission-enabling technology is required for either the instruments or the spacecraft, the accelerated schedule shown here could be implemented.

		Instruments On & Transmitting (Peak)	Nominal Mission Mode (Day)	Nominal Mission Mode (Night)	Safe Mode
	Margin %	Peak	Avg. Power	Avg. Power	Avg. Power
<b>Total Power</b>		182.2	132.9	141.9	143.2
<b>Instrument Totals &amp; Margin</b>		38.64	38.64	38.64	0
Margin	.20	20	6.44	6.44	0
Hot Plasma (2@7W)		14	14	14	0
Energetic Particles (1@2W)		2	2	2	0
3-Axis Magnetometer (1@1.2W)		1.2	1.2	1.2	0
Search coil		0.4	0.4	0.4	0
Electric Field		15	15	15	0
<b>Spacecraft Loads--Margined</b>		143.2	93.8	102.8	143.2
Power		11.0	11.0	11.0	11.0
<b>PSE</b> 92% Efficient (120W Load)	10.0	11.0	11.0	11.0	11.0
Electrical		6.2	6.2	6.2	6.2
<b>PSDU</b> (2.2% of 120W Load)	10.0	2.9	2.9	2.9	2.9
<b>Harness</b> (2.5% of 120W Load)	10.0	3.3	3.3	3.3	3.3
Attitude Control		10.4	10.4	10.4	10.4
<b>Digital Sun Sensors:</b>					
<b>Earth Sensor:</b> Ithaco Steerable Horizon Crossing Indicator (SHCI) (7.5W)	1.0	2.8	2.8	2.8	2.8
<b>Nutation Damper:</b> Not Required	1.0	0.0	0.0	0.0	0.0
<b>ACE:</b> Functions Reside In CDH		0.0	0.0	0.0	0.0
Command & Data Handling		37.8	37.8	37.8	37.8
<b>Processor:</b> Primary @ 16W; Redundant @8W	20.0	37.8	37.8	37.8	37.8
Communications		66.8	26.5	26.5	66.8
<b>Small Deep Space Transponder</b> (12.7W)	10	14.0	14.0	14.0	14.0
<b>TWTA</b> (20W RF; 40W Power) On When Transmitting	10	44.0	3.7	3.7	44.0
<b>IRAS</b> ranging (8W)	10	8.8	8.8	8.8	8.8
Thermal		9.0	0.0	9.0	9.0
Propulsion & Battery Heaters		9.0	0.0	9.0	9.0
Propulsion		2.02	2.02	2.02	2.02
Transducers, Electronics	1	2.02	2.02	2.02	2.02

**Table 8.5.** MMS power budget.



## Appendix: Selected References



## Introduction

- dePater, I., M. Schulz, and S. H. Brecht, Synchrotron evidence for Amalthea's influence on Jupiter's electron radiation belt. *J. Geophys. Res.*, **102**, 22043, 1997.
- Fälthammar, C.-G., S.-I. Akasofu, and H. Alfvén, The significance of magnetospheric research for progress in astrophysics. *Nature*, **275**, 185, 1978.
- Wainscoat, R. J., and K. Kormendy, A new color image of the Crab Nebula. *PASP*, **109**, 279, 1997.

## Reconnection

- Anderson, B. J., et al., Relationships between plasma depletion and subsolar reconnection. *J. Geophys. Res.*, **102**, 9531, 1997.
- Baker, D. N., et al., Neutral line view of substorms: past results and present view. *J. Geophys. Res.*, **101**, 12975, 1996.
- Büchner, L., et al., Three-dimensional reconnection in the Earth's magnetotail: simulations and observations. in *Geospace Mass and Energy Flow: Results from the International Solar-Terrestrial Physics* program, edited by J. L. Horowitz et al., Geophysical Monograph 104, p. 313, 1998.
- Cowley, S. W. H., The causes of convection in the Earth's magnetosphere: A review of developments during the IMS. *Rev. Geophys. Space Phys.*, **20**, 531, 1982.
- Crooker, N. U., The half-wave rectifier response of the magnetosphere and antiparallel merging. *J. Geophys. Res.*, **85**, 575, 1980.
- Crooker, N. U., Morphology of magnetic merging at the magnetopause, *JATP*, **52**, 1123, 1990.
- Crooker, N. U., G. L. Siscoe, and F. R. Toffoletto, A tangent subsolar merging line. *J. Geophys. Res.*, **95**, 3787, 1990.
- Crooker, N. U., and F. R. Toffoletto, Global aspects of magnetopause-ionosphere coupling: review and synthesis. in *Physics of the Magnetopause*, edited by P. Song et al., Geophysical Monograph 90, pp. 363-370, American Geophysical Union, Washington D. C., 1995.
- Elphic, R. C., Observations of flux transfer events: A review. in *Physics of the Magnetopause*, edited by P. Song et al., Geophysical Monograph 90, p. 225, American Geophysical Union, Washington D.C., 1995.
- Gosling, J. T., et al., Accelerated plasma flows at the near-tail magnetopause. *J. Geophys. Res.*, **91**, 3029, 1986.
- Hesse, M., The magnetotail's role in magnetospheric dynamics: engine or exhaust pipe. *Rev. Geophys.*, Supplement: U. S. National Report to the IUGG, 675, 1995.
- Hesse, M., et al., The diffusion region in collisionless magnetic reconnection. *Phys. Plasmas*, **6**, 1781, 1999.
- Hesse, M., and D. Winske, Electron dissipation in collisionless magnetic reconnection. *J. Geophys. Res.*, **103**, 26479, 1998.
- Kessel, R. L., et al., Evidence of high-latitude reconnection during northward IMF: Hawkeye observations. *Geophys. Res. Lett.*, **23**, 583, 1996.
- LaBelle-Hamer, A. L., et al., Magnetic reconnection in the presence of sheared flow and density asymmetry: applications to the Earth's magnetopause. *J. Geophys. Res.*, **100**, 11891, 1995.
- Le, G., et al., Flux transfer events: spontaneous or driven?, *Geophys. Res. Lett.*, **20**, 791, 1993.
- Lockwood, M., and M. N. Wild, On the quasi-periodic nature of flux transfer events. *J. Geophys. Res.*, **98**, 5935, 1993.
- Lockwood, M., et al., Modelling signatures of pulsed magnetopause reconnection in cusp ion dispersion signatures seen at middle latitudes. *Geophys. Res. Lett.*, **25**, 591, 1998.
- Luhmann, J. G., et al., Patterns of potential magnetic field merging sites in the dayside magnetosphere. *J. Geophys. Res.*, **89**, 1739, 1984.
- Nagai, T., et al., Structure and dynamics of magnetic reconnection for substorm onsets with Geotail observations. *J. Geophys. Res.*, **103**, 4419, 1998.
- Nishida, A., et al., GEOTAIL observations on the reconnection process in the distant tail in geographically active times. *Geophys. Res. Lett.*, **22**, 2453, 1995.
- Nishida, A., and T. Ogino, Convection and reconnection in the Earth's magnetotail, in *New Perspectives on the Earth's Magnetotail*, edited by A. Nishida et al., Geophysical Monograph 105, pp. 61-76, American Geophysical Union, Washington D. C., 1998.
- Onsager, T. G., et al., Low-altitude observations and modeling of quasi-steady magnetopause reconnection. *J. Geophys. Res.*, **100**, 11831, 1995.
- Phan, T.-D., Paschmann, G., and B. U. Ö. Sonnerup, Low-latitude dayside magnetopause and boundary layer for high magnetic shear 2. Occurrence of magnetic reconnection. *J. Geophys. Res.*, **101**, 7817, 1996.

- Scholer, M., Models of flux transfer events, in *Physics of the Magnetopause*, edited by P. Song et al., Geophysical Monograph 90, pp. 235-245. American Geophysical Union, Washington D. C., 1995.
- Scurry, L., C. T. Russell, and J. T. Gosling, Geomagnetic activity and the beta dependence of the dayside reconnection rate, *J. Geophys. Res.*, **89**, 14811, 1994.
- Shay, M. A., and J. F. Drake, The role of electron dissipation on the rate of collisionless magnetic reconnection, *Geophys. Res. Lett.*, **25**, 3759, 1998.
- Sonnerup, B. U. Ö., Magnetopause reconnection rate, *J. Geophys. Res.*, **79**, 1546, 1974.
- Winglee, R. M., et al., Flux rope structures in the magnetotail: Comparison between Wind/Geotail observations and global simulations, *J. Geophys. Res.*, **103**, 135, 1998.
- White, W. W., et al., The magnetospheric sash and the cross-tail S, *Geophys. Res. Lett.*, **25**, 1605, 1998.

### Charged Particle Acceleration

- Angelopoulos, V., et al., Bursty bulk flows in the inner central plasma sheet, *J. Geophys. Res.*, **97**, 4027, 1992.
- Angelopoulos, V., et al., Tailward progression of magnetotail acceleration centers: relationship to substorm current wedge, *J. Geophys. Res.*, **101**, 24599, 1996.
- Ashour-Abdalla, M., et al., Shaping of the magnetotail from the mantle: global and local structuring, *J. Geophys. Res.*, **98**, 5651, 1993.
- Ashour-Abdalla, M., et al., The mosaic structure of plasma bulk flows in the Earth's magnetotail, *J. Geophys. Res.*, **100**, 19191, 1995.
- Baker, D. N., et al., Deep dielectric charging effects due to high energy electrons in Earth's outer magnetosphere, *J. Electrostat.*, **20**, 3, 1987.
- Baker, D. N., et al., Relativistic electron acceleration and decay time scales in the inner and outer radiation belts: SAMPEX, *Geophys. Res. Lett.*, **21**, 409, 1994.
- Baker, D. N., et al., A strong CME-related magnetic cloud interaction with the Earth's magnetosphere: ISTP observation of rapid relativistic electron acceleration on May 15, 1997, *Geophys. Res. Lett.*, **25**, 2975, 1998.
- Baumjohann, W., G. Paschmann, and H. Lühr, Characteristics of high-speed ion flows in the plasma sheet, *J. Geophys. Res.*, **95**, 3801, 1990.
- Birn, J., and M. Hesse, Particle acceleration in the dynamic magnetotail: orbits in self-consistent three-dimensional MHD fields, *J. Geophys. Res.*, **99**, 109, 1994.
- Birn, J., et al., Substorm ion injections: Geosynchronous observations and test particle orbits in three-dimensional dynamics MHD fields, *J. Geophys. Res.*, **102**, 2325, 1997.
- Birn, J., et al., Substorm electron injections: Geosynchronous observations and test particle simulations, *J. Geophys. Res.*, **103**, 9235, 1998.
- Blake J. B., et al., Injection of electrons and protons with energies of tens of MeV into L<3 on March 24, 1991, *Geophys. Res. Lett.*, **19**, 821, 1992.
- Blake J. B., et al., Correlation of changes in the outer-zone relativistic-electron population with upstream solar wind and magnetic field measurements, *Geophys. Res. Lett.*, **24**, 927, 1997.
- Büchner, J., Heavy ion acceleration by reconnection in the magnetotail: theory and GEOTAIL observations, in *New Perspectives on the Earth's Magnetotail*, edited by A. Nishida et al., Geophysical Monograph 105, p. 181. American Geophysical Union, 1998.
- Chang, S. W., et al., Cusp energetic ions: A bow shock source, *Geophys. Res. Lett.*, **25**, 3729, 1998.
- Chen, J. and T. A. Fritz, Correlation of cusp MeV helium with turbulent ULF power spectra, *Geophys. Res. Lett.*, **25**, 4113, 1998.
- Chen, J., et al., Cusp energetic particle events: Implications for a major acceleration region of the magnetosphere, *J. Geophys. Res.*, **103**, 69, 1998.
- Elkington, S. R., M. K. Hudson, and A. A. Chan, Acceleration of relativistic electrons via drift-resonant interaction with toroidal-mode Pc-5 ULF oscillations, *Geophys. Res. Lett.*, in press, 1999.
- Horne, R. B., and R. M. Thorne, Potential waves for relativistic electron scattering and stochastic acceleration during magnetic storms, *Geophys. Res. Lett.*, **25**, 3011, 1998.
- Hudson, M. K., et al., Simulation of Proton Radiation Belt Formation During the March 24, 1991 SSC, *Geophys. Res. Lett.*, **22**, 291, 1995.
- Hudson, M. K., Simulation of radiation belt dynamics driven by solar wind variations, in *Sun-Earth Plasma Connections*, edited by J. L. Burch et al., p. 171, Geophysical Monograph 109, American Geophysical Union, 1999.

- Li, X., et al., Simulation of the prompt energization and transport of radiation particles during the March 23, 1991 SSC, *Geophys. Res. Lett.*, **20**, 2423, 1993.
- Li, X., et al., Are energetic electrons in the solar wind the source of the outer radiation belt? *Geophys. Res. Lett.*, **24**, 923, 1997.
- Li, X., et al., Simulation of dispersionless injections and drift echoes of energetic electrons associated with substorms, *Geophys. Res. Lett.*, **25**, 3763, 1998.
- Liu, W. W., G. Rostoker, and D. N. Baker, Internal acceleration of relativistic electrons by large-amplitude ULF pulsations, *J. Geophys. Res.*, **104**, 17391, 1999.
- Lyons, L. R., and T. W. Speiser, Evidence for current sheet acceleration in the geomagnetic tail, *J. Geophys. Res.*, **87**, 2276, 1982.
- Parks, G. et al., New observations of ion beams in the plasma sheet boundary layer, *Geophys. Res. Lett.*, **25**, 3285, 1998.
- Scholer, M., Energetic ions and electrons and their acceleration processes in the magnetotail, in *Magnetic Reconnection in Space and Laboratory Plasmas*, edited by E. W. Hones, Jr., Geophysical Monograph 30, p. 216, American Geophysical Union, 1984
- Selesnick, R. S., and J. B. Blake, Dynamics of the outer radiation belt, *Geophys. Res. Lett.*, **24**, 1347, 1997.
- Takahashi, K., and E. W. Hones, Jr., ISEE 1 and 2 observations of ion distributions at the plasma sheet-tail lobe boundary, *J. Geophys. Res.*, **93**, 8558, 1988.
- Trattner, K. J., S. A. Fuselier, W. K. Peterson, and S. W. Chang, Comment on "Correlation of cusp MeV helium with turbulent ULF power spectra and its implications" by J. Chen and T. A. Fritz, *Geophys. Res. Lett.*, **25**, 1361, 1999

## Turbulence

- Anderson, B. J., ULF signals observed near the magnetopause, in *Physics of the Magnetopause*, edited by P. Song et al., Geophysical Monograph 90, p. 269, American Geophysical Union, Washington D.C., 1995.
- Angelopoulos, V., et al., Bursty bulk flows in the inner central plasma sheet, *J. Geophys. Res.*, **97**, 4027, 1992.
- Baker, D. N., et al., Neutral line model of substorms: Past results and present view, *J. Geophys. Res.*, **101**, 12975, 1996.
- Birn, J., and M. Hesse, Details of current disruption and diversion in simulations of magnetotail dynamics, *J. Geophys. Res.*, **101**, 15345, 1996.
- Borovsky, J. E., et al., The Earth's plasma sheet as a laboratory for flow turbulence in high- $\beta$  MHD, *J. Plasma Physics*, **57**, 1, 1997.
- Bowling, S. B. Transient occurrence of magnetic loops in the magnetotail, *J. Geophys. Res.*, **80**, 4741, 1975.
- Cattell, C. A., and F. S. Mozer, Substorm-associated lower hybrid waves in the plasma sheet observed by ISEE 1, in *Magnetotail Physics*, edited by A.T.Y. Lui, p. 119, Johns Hopkins Univ. Press, Baltimore, MD, 1987.
- Chang, T. S., Low dimensional behaviour and symmetry breaking of stochastic systems near criticality - can these effects be observed in space and in the laboratory? *IEEE Trans. Plasma Sci.*, **20**, 691, 1992.
- Cheng, C. Z., and A. T. Y. Lui, Kinetic ballooning instability for substorm onset and current disruption observed by AMPTE/CCE, *Geophys. Res. Lett.*, **25**, 4091, 1998.
- Coroniti, F. V., et al., Variability of plasma sheet dynamics, *J. Geophys. Res.*, **85**, 2957, 1980.
- Coroniti, F. V., and K. B. Quest, Nonlinear evolution of magnetopause tearing modes, *J. Geophys. Res.*, **89**, 137, 1984.
- Crooker, N. U., G. L. Siscoe, and R. B. Geller, Persistent pressure anisotropy in the subsonic magnetosheath region, *Geophys. Res. Lett.*, **3**, 65, 1976.
- Crooker, N. U., and G. L. Siscoe, A mechanism for pressure anisotropy and mirror instability in the dayside magnetosheath, *J. Geophys. Res.*, **82**, 185, 1977.
- Denton, R. E., et al., Low-frequency magnetic fluctuation spectra in the magnetosheath and plasma depletion layer, *J. Geophys. Res.*, **99**, 5893, 1994.
- Fairfield, D. H., Magnetic fields of the magnetosheath, *Rev. Geophys.*, **14**, 117, 1976.
- Galeev, A. A., M. M. Kuznetsova, and L. M. Zeleny, Magnetopause stability threshold for patchy reconnection, *Space Sci. Rev.*, **44**, 1, 1986.
- Gary, S. P., et al., Proton anisotropies upstream of the magnetopause, in *Physics of the Magnetopause*, p. 123, American Geophysical Union, Washington D.C., 1995.
- Gleaves, D. G., and D. J. Southwood, Magnetohydrodynamic fluctuations in the Earth's magnetosheath at 1500 LT: ISEE 1 and ISEE 2, *J. Geophys. Res.*, **96**, 129, 1991.
- Gurnett, D. A., et al., Plasma wave turbulence at the magnetopause: Observations from ISEE 1 and 2, *J. Geophys. Res.*, **84**, 7034, 1979.

- Hau, L.-N., and B. U. Ö. Sonnerup, Two-dimensional coherent structures in the magnetopause: Recovery of static equilibria from single-spacecraft data, *J. Geophys. Res.*, **104**, 6899, 1999.
- Hones, E. W., et al., Further determination of the characteristics of magnetospheric plasma vortices with ISEE 1 and 2, *J. Geophys. Res.*, **86**, 814, 1981.
- Huba, J. D., et al., The lower-hybrid-drift instability as a source of anomalous resistivity for magnetic field line reconnection, *Geophys. Res. Lett.*, **4**, 125, 1977.
- Kivelson, M. G., and S.-H. Chen, The magnetopause: Surface waves and instabilities and their possible dynamical consequences, in *Physics of the Magnetopause*, *Geophys. Monogr.* 90, eds. P. Song, B.U.Ö. Sonnerup and M.F. Thomsen, p. 257, AGU, Washington D.C., 1995.
- Kuznetsova, M. M., and L. M. Zelenyi, The theory of FTE stochastic percolation model, in *Physics of Magnetic Flux Ropes*, edited by C. T. Russell et al., Geophysical Monograph 58, p. 473 American Geophysical Union, 1990.
- LaBelle, J., and R. A. Treumann, Plasma waves at the day-side magnetopause, *Space Sci. Rev.*, **47**, 175, 1988.
- Lui, A. T. Y., Characteristics of the cross-tail current in the Earth's magnetotail, in *Magnetospheric Currents*, edited by T. A. Potemra, Geophysical Monograph 28, p. 158, American Geophysical Union, 1984.
- Lui, A. T. Y., Current disruption in the Earth's magnetosphere: Observations and models, *J. Geophys. Res.*, **101**, 13067, 1996.
- Lui, A. T. Y., and A.-H. Najmi, Time-frequency decomposition of signals in a current disruption event, *Geophys. Res. Lett.*, **24**, 3157, 1997.
- Miura, A. Self-organization in the two-dimensional magnetohydrodynamic transverse Kelvin-Helmholtz instability, *J. Geophys. Res.*, **104**, 395, 1999.
- Ogilvie, K. W., and R. J. Fitzenreiter, The Kelvin-Helmholtz instability at the magnetopause and inner boundary layer surface, *J. Geophys. Res.*, **94**, 15,113, 1989.
- Phan, T.-D., and G. Paschmann, The magnetosheath region adjacent to the dayside magnetopause, in *Physics of the Magnetopause*, *Geophys. Monogr.* 90, eds. P. Song, B.U.Ö. Sonnerup, and M.F. Thomsen, p. 115, AGU, Washington D.C., 1995.
- Prichett, P. L., et al., Three-dimensional stability of thin quasi-neutral current sheet, *J. Geophys. Res.*, **101**, 27413, 1996.
- Quest, K. B., and F. V. Coroniti, Tearing at the dayside magnetopause, *J. Geophys. Res.*, **86**, 3289, 1982.
- Rezeau, L., A. Roux, and C. T. Russell, Characterization of small-scale structures at the magnetopause from ISEE measurements, *J. Geophys. Res.*, **98**, 179, 1993.
- Russell, C. T., The structure of the magnetopause, in *Physics of the Magnetopause*, edited by P. Song et al., Geophysical Monograph 90, p. 81, American Geophysical Union, Washington D.C., 1995.
- Schlichting, H., *Boundary-Layer Theory*, 748 pp., McGraw-Hill, New York, 1968.
- Sibeck, D. G., A model for the transient magnetospheric response to sudden solar wind dynamic pressure variations, *J. Geophys. Res.*, **95**, 3755, 1990.
- Sibeck, D. G., The magnetospheric response to foreshock pressure pulses, in *Physics of the Magnetopause*, edited by P. Song et al., Geophysical Monograph 90, p. 293, American Geophysical Union, Washington D.C., 1995.
- Song, P., C. T. Russell, and C. Y. Huang, Wave properties near the subsolar magnetopause: Pc 1 waves in the sheath transition layer, *J. Geophys. Res.*, **98**, 5907, 1993.
- Sonnerup, B. U. Ö., and M. Guo, Magnetopause transects, *Geophys. Res. Lett.*, **23**, 3679, 1996.
- Sundaram, A. K., and D. H. Fairfield, The tearing instabilities driven by lower hybrid waves in the current sheet, *J. Geophys. Res.*, **101**, 24919, 1996.
- Takahashi, K., et al., Disruption of the magnetotail current sheet observed by AMPTE/CCE, *Geophys. Res. Lett.*, **14**, 1019, 1987.
- Treumann, R. A., J. LaBelle, and T. M. Bauer, Diffusion processes: An observational perspective, in *Physics of the Magnetopause*, edited by P. Song et al., Geophysical Monograph 90, p. 331, American Geophysical Union, Washington D.C., 1995.
- Walthour, D. W., et al., Remote sensing of two-dimensional magnetopause structures, *J. Geophys. Res.*, **98**, 1489, 1993.
- Walthour, D. W., et al., Double vision: Remote sensing of a flux transfer event with ISEE 1 and 2, *J. Geophys. Res.*, **99**, 8555, 1994.
- Yoon, P. H., and A. T. Y. Lui, Nonlinear analysis of generalized cross-field current instability, *Phys. Fluids B*, **5**, 836-853, 1993.
- Zhu, Z., and R. M. Winglee, Tearing instability, flux rope, and the kinetic current sheet kink instability in the Earth's magnetotail: A three-dimensional perspective from particle simulation, *J. Geophys. Res.*, **101**, 4885, 1996.



# REPORT DOCUMENTATION PAGE

*Form Approved*  
OMB No. 0704-0188

Public reporting burden for this collection of information is estimated to average 1 hour per response, including the time for reviewing instructions, searching existing data sources, gathering and maintaining the data needed, and completing and reviewing the collection of information. Send comments regarding this burden estimate or any other aspect of this collection of information, including suggestions for reducing this burden, to Washington Headquarters Services, Directorate for Information Operations and Reports, 1215 Jefferson Davis Highway, Suite 1204, Arlington, VA 22202-4302, and to the Office of Management and Budget, Paperwork Reduction Project (0704-0188), Washington, DC 20503.

<b>1. AGENCY USE ONLY</b> <i>(Leave blank)</i>	<b>2. REPORT DATE</b> December 1999	<b>3. REPORT TYPE AND DATES COVERED</b> Technical Memorandum	
<b>4. TITLE AND SUBTITLE</b> The Magnetospheric Multiscale Mission...Resolving Fundamental Processes in Space Plasmas		<b>5. FUNDING NUMBERS</b>  Code 695	
<b>6. AUTHOR(S)</b> S. Curtis			
<b>7. PERFORMING ORGANIZATION NAME(S) AND ADDRESS (ES)</b>  Goddard Space Flight Center Greenbelt, Maryland 20771		<b>8. PERFORMING ORGANIZATION REPORT NUMBER</b>  2000-01130-0	
<b>9. SPONSORING / MONITORING AGENCY NAME(S) AND ADDRESS (ES)</b>  National Aeronautics and Space Administration Washington, DC 20546-0001		<b>10. SPONSORING / MONITORING AGENCY REPORT NUMBER</b> TM—2000—209883	
<b>11. SUPPLEMENTARY NOTES</b>			
<b>12a. DISTRIBUTION / AVAILABILITY STATEMENT</b> Unclassified—Unlimited Subject Category: 88 Report available from the NASA Center for AeroSpace Information, 7121 Standard Drive, Hanover, MD 21076-1320. (301) 621-0390.		<b>12b. DISTRIBUTION CODE</b>	
<b>13. ABSTRACT</b> <i>(Maximum 200 words)</i> The Magnetospheric Multiscale (MMS) mission is a multiple-spacecraft Solar-Terrestrial Probe designed to study the microphysics of magnetic reconnection, charged particle acceleration, and turbulence in key boundary regions of Earth's magnetosphere. These three processes, which control the flow of energy, mass, and momentum within and across plasma boundaries, occur throughout the universe and are fundamental to our understanding of astrophysical and solar system plasmas. Only in Earth's magnetosphere, however, are they readily accessible for sustained study through in-situ measurement. MMS will employ five co-orbiting spacecraft, identically instrumented to measure electric and magnetic fields, plasmas, and energetic particles. The initial parameters of the individual spacecraft orbits will be designed so that the spacecraft formation will evolve into a three-dimensional configuration near apogee, allowing MMS to differentiate between spatial and temporal effects and to determine the three-dimensional geometry of plasma, field, and current structures. In order to sample all of the magnetospheric boundary regions, MMS will employ a unique four-phase orbital strategy involving carefully sequenced changes in the local time and radial distance of apogee and, in the third phase, a change in orbit inclination from 10° to 90°. The nominal mission operational lifetime is two years. Launch is currently scheduled for 2006.			
<b>14. SUBJECT TERMS</b> Magnetospheric Multiscale mission, MMS, magnetic reconnection, charged particle acceleration, turbulence		<b>15. NUMBER OF PAGES</b> 35	<b>16. PRICE CODE</b>
<b>17. SECURITY CLASSIFICATION OF REPORT</b> Unclassified	<b>18. SECURITY CLASSIFICATION OF THIS PAGE</b> Unclassified	<b>19. SECURITY CLASSIFICATION OF ABSTRACT</b> Unclassified	<b>20. LIMITATION OF ABSTRACT</b> UL







---